Supplementary Information

Thermoresponsive Fluorescent Polymers: Influence of Size, Composition, and Architecture

Konpal Raheja, Sophia Beilharz, Ajitesh Lalam, Md. Bablu Hasan, Divita Mathur, Metin Karayilan*

* Corresponding Author: metin.karayilan@case.edu

Table of Contents

1. Materials and Equipment

Materials

Di(ethylene glycol) methyl ether methacrylate (DEGMA, Sigma-Aldrich, 95%) and oligo(ethylene glycol) methyl ether methacrylate (OEGMA, M_n=500 g/mol, Sigma-Aldrich) were purified through a short basic alumina column to remove inhibitors. *N*-Isopropylacrylamide (NIPAM, TCI, >98%) was recrystallized from hexanes. 2,2'-Azobis(2-methylpropionitrile) (AIBN, Sigma-Aldrich, 98%) was recrystallized from methanol. 4-Cyano-4-(((dodecylthio)carbonothioyl)thio) pentanoic acid (Chain transfer agent, CTDPA, Boron Molecular, 99%), fluorescein o-acrylate (FluA, Sigma-Aldrich, 95%), fluorescein (free acid, Flu, Sigma-Aldrich, 95%), 4,4'-azobis(4-cyanovaleric acid) (ACVA, Sigma-Aldrich, 98%), *N, N*-dimethylformamide (DMF, Fisher Scientific, ACS Grade), toluene (PhMe, Fisher Scientific, ACS Grade), chloroform (Fisher Scientific, ACS Grade), hexanes (Fisher Scientific, ACS Grade), methanol (Fisher Scientific, HPLC Grade), *N, N*-dimethylformamide (DMF, HPLC Grade, Alfa Aesar, 99.7+%), and deuterated chloroform ($CDCl_3$, 99.8+ atom % D contains 0.02-0.04 v/v% TMS or no TMS added, ThermoScientific) were used as received. Acetate buffer for pH 3 and 5, phosphate-buffered saline (PBS) for pH 7.4, and ammonium hydroxide (NH_4OH) solution for pH 9 (predominantly KCl-based) and pH 11 were used to study pH-dependence.

Equipment

Nuclear Magnetic Resonance (NMR) spectra were recorded on Bruker AscendTM 500. Size Exclusion Chromatography with multi-angle light scattering (SEC-MALS) analyses were carried out on 1260 Infinity II GPC/SEC System (Agilent Technologies). HPLC-grade DMF was used as the eluent with a flow rate of 0.6 mL/min at room temperature 25 °C. The SEC was equipped with a Wyatt Optilab T-rEX refractive index detector and a Wyatt Dawn Heleos II 18-angle MALS detector. The refractive index and light-scattering detectors operated at an optical wavelength of 658 nm (dn/dC = 0.071 for NIPAM systems and 0.040 for PEGMA systems). The cloud point temperature (T_{cp}) analyses were recorded on Cary 3500 Peltier UV-Vis Spectrometer (Agilent Technologies) at a wavelength of 600 nm and ramp rate of 0.5 °C. T_{cp} was determined at 90% transmission. UV-Vis absorption and transmittance spectra were recorded using a Cary Series UV-Vis-NIR spectrophotometer (Agilent Technologies). Fluorescence spectra were obtained using a Cary Eclipse Fluorescence Spectrophotometer (Agilent Technologies). All measurements were performed on samples prepared in PBS at pH 7.4 at a concentration of 0.1 mg/mL for both UV-Vis and fluorescence analyses.

Temperature-based absorbance and fluorescence measurements were performed using a Tecan SparkControl Magellan microplate reader, operated via SparkControl software. The instrument was equipped with monochromator-based excitation and emission optics and integrated temperature control. Measurements were conducted using black, flat-bottom 96-well microplates (Thermo Fisher Scientific, Nunclon™), with a sample volume of 50 µL per well. Temperature-

dependent experiments were carried out using a kinetic measurement mode with active temperature control. The temperature was varied from 18 to 42 °C over a period of 1 hour, with data acquisition at 1-minute intervals. Absorbance spectra were collected in the wavelength range of 400-800 nm with a step size of 2 nm, using a settle time of 50 ms and one flash per data point. Fluorescence measurements were performed in top-reading emission scan mode, using monochromator-based excitation at 450 nm (bandwidth 10 nm). Emission spectra were recorded with a step size of 2 nm and an emission bandwidth of 10 nm.

Dynamic Light Scattering (DLS) measurements were performed on a Mobius (Wyatt Technology Corporation), under controlled temperature conditions. The sample temperature was increased at a rate of 0.1 °C/min over the specified range. At each temperature, a 2 min delay was used to ensure the sample viscosity was equilibrated before measurements were taken. The polymer solutions were filtered through 0.45 µm PES filters before the measurements. Data collection and analysis were carried out using the DYNAMICS software package (Wyatt Technology Corporation).

2. PNIPAM-based Linear Thermoresponsive Fluorescent Polymers: Synthesis and Characterization

2.1. Linear P(NIPAM-*co*-FluA), (Feed ratio = 95:5)

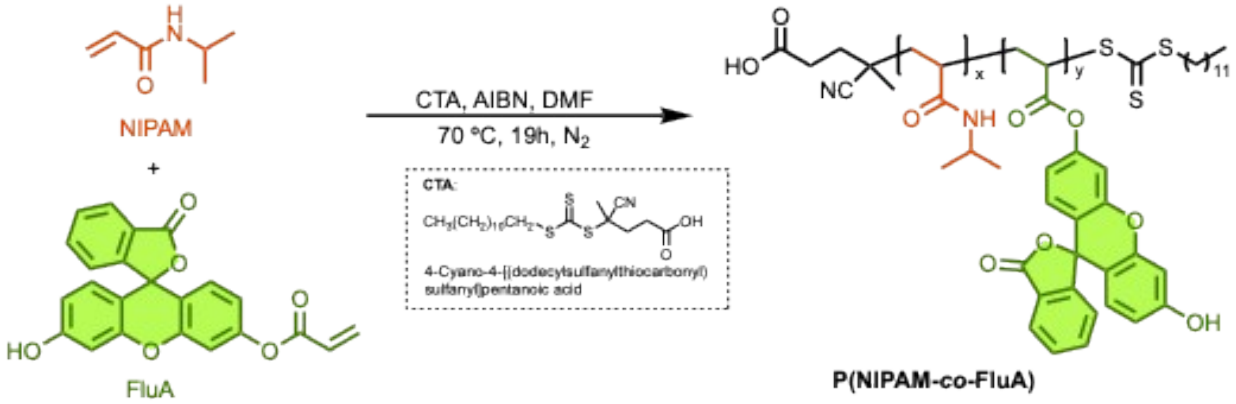

Scheme S1. Synthesis of linear P(NIPAM-*co*-FluA) (feed ratio = 95:5) via RAFT polymerization.

Recrystallized NIPAM (0.5 g, 4.42 mmol), FluA (89.85 mg, 0.23 mmol), CTDPA (1.9 mg, 0.005 mmol), and AIBN (0.75 mg, 0.005 mmol) were dissolved in DMF (1.5 mL) in a 25mL Schlenk flask equipped with a Teflon-coated stir bar. The reaction mixture was deoxygenated by purging and sparging with N_2 for 10 min. After sparging, the Schlenk flask with the reaction mixture was heated at 70 °C for 19 hours. The obtained copolymer was purified by dissolving in methanol and precipitating in hexanes three times and then dried under vacuum for further characterization, with an isolated yield of 0.46 g. Actual Composition = 94.8:5.2 by ^{1}H NMR Spectroscopy; SEC-MALS (DMF) characterization: M_n = 342.4 kDa, Đ = 2.5.

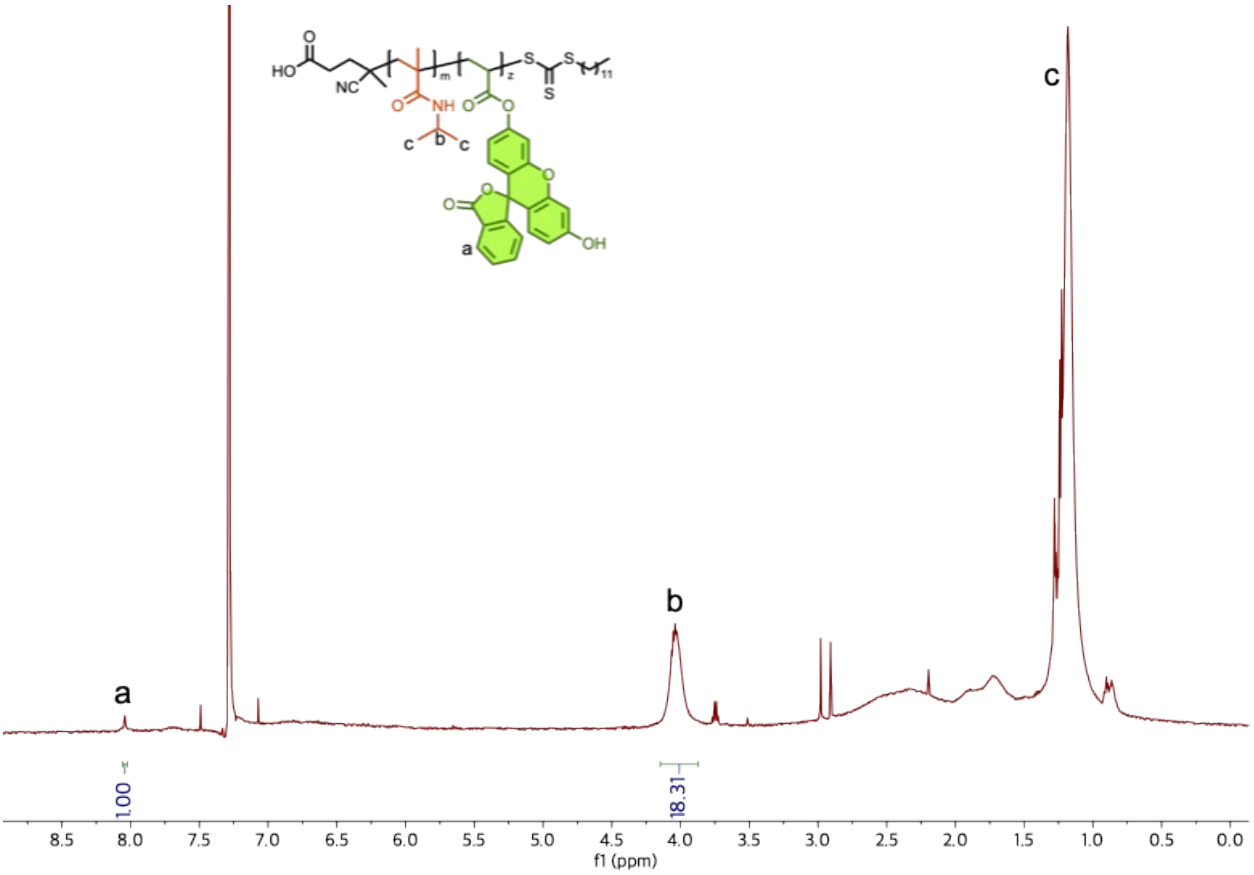

Figure S1. ^{1}H NMR spectrum of linear P(NIPAM$_{94.8}$-*co*-FluA$_{5.2}$) synthesized via conventional RAFT polymerization in $CDCl_3$.

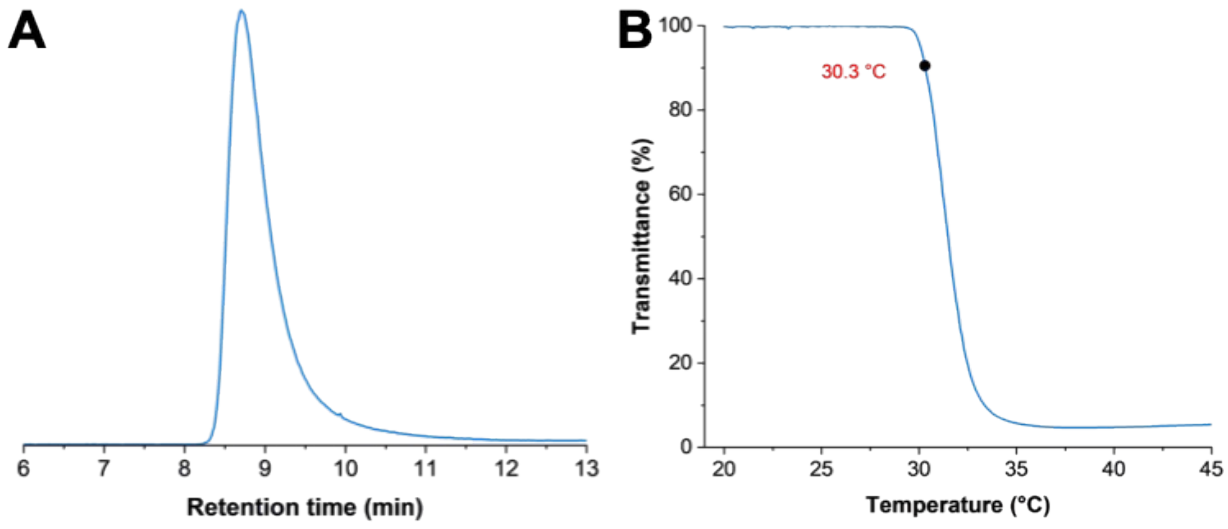

Figure S2. **(A)** SEC-MALS (DMF) trace and **(B)** cloud point temperature profile at 10 mg/mL of linear P(NIPAM$_{94.8}$-*co*-FluA$_{5.2}$) synthesized via conventional RAFT polymerization.

2.2. Linear P(NIPAM-*co*-FluA), (Feed ratio = 99:1)

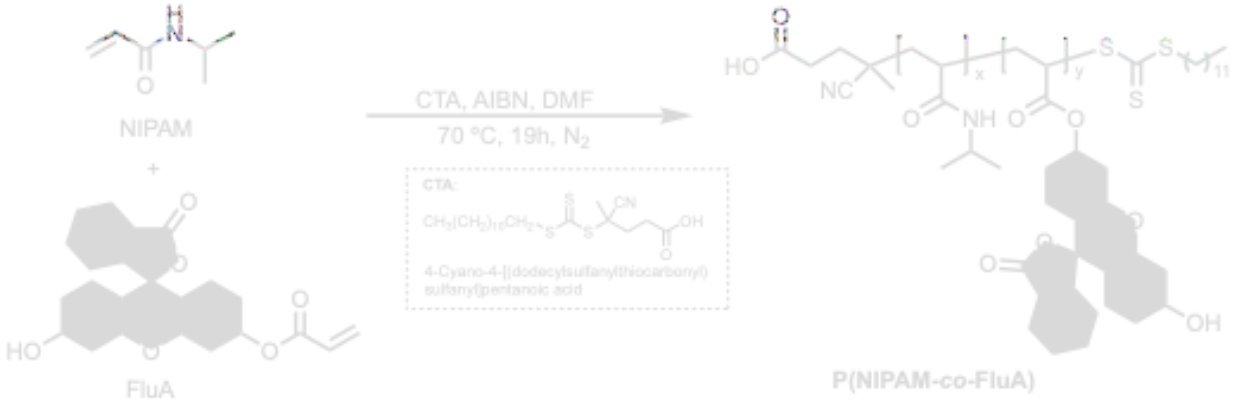

Scheme S2. Synthesis of linear P(NIPAM-*co*-FluA) (feed ratio = 99:1) via RAFT polymerization.

Recrystallized NIPAM (1.00 g, 8.84 mmol), FluA (34.1 mg, 0.09 mmol), CTDPA (3.4 mg, 0.009 mmol), and AIBN (1.9 mg, 0.009 mmol) were dissolved in DMF (1 mL) in a 25mL Schlenk flask equipped with a Teflon-coated stir bar. The reaction mixture was deoxygenated by purging and sparging with N_2 for 10 min. After sparging, the Schlenk flask with the reaction mixture was heated at 70 °C for 19 hours. The obtained copolymer was purified by dissolving in methanol and precipitating in hexanes three times and then dried under vacuum for further characterization, with an isolated yield of 0.83 g. Actual Composition = 96:4 by ^{1}H NMR Spectroscopy; SEC-MALS (DMF) characterization: M_n = 273.4 kDa, Đ = 1.4.

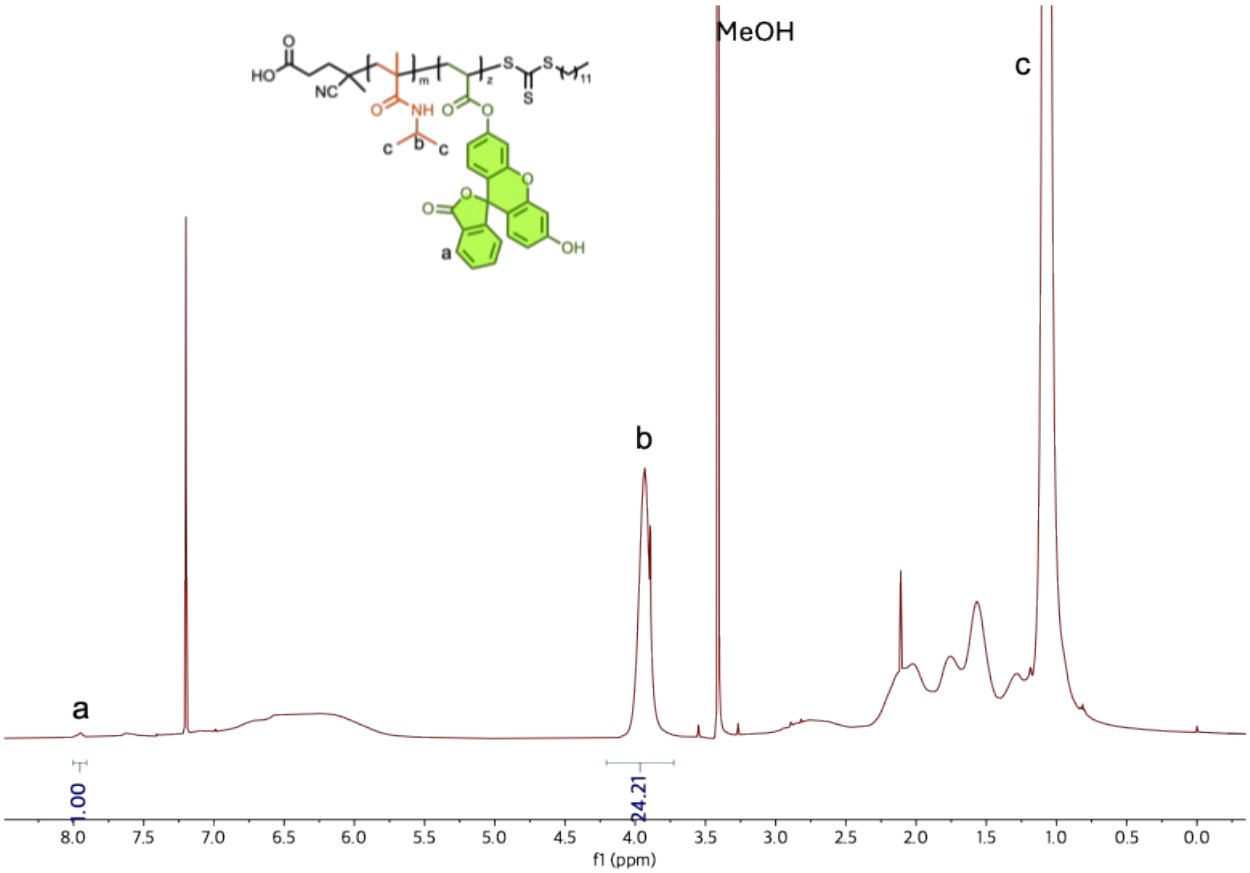

Figure S3. ^{1}H NMR spectrum of linear P(NIPAM$_{96}$-*co*-FluA$_4$) synthesized via conventional RAFT polymerization in $CDCl_3$.

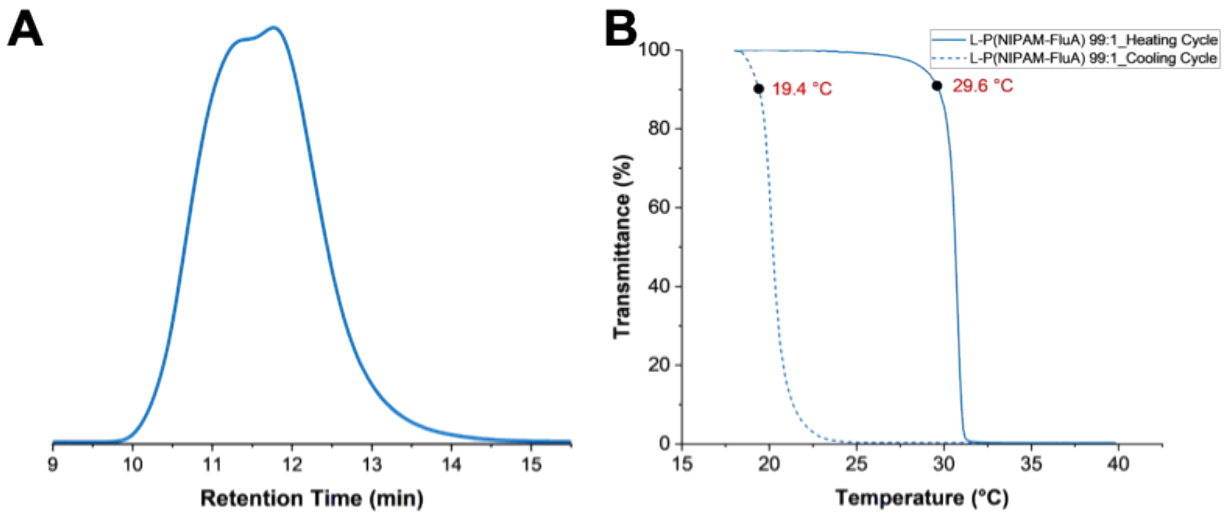

Figure S4. **(A)** SEC-MALS (DMF) trace and **(B)** cloud point temperature profile at 10 mg/mL of linear P(NIPAM$_{96}$-*co*-FluA$_4$) synthesized via conventional RAFT polymerization.

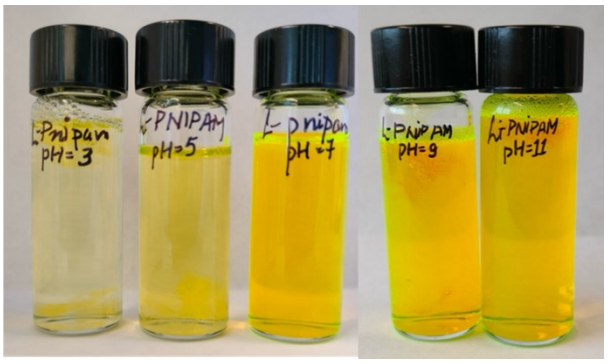

Figure S5. Visual comparison of linear P(NIPAM$_{96}$-*co*-FluA$_4$) solubility/behavior in pH 3, 5, 7.4, 9, and 11 buffer solution at 5mg/mL.

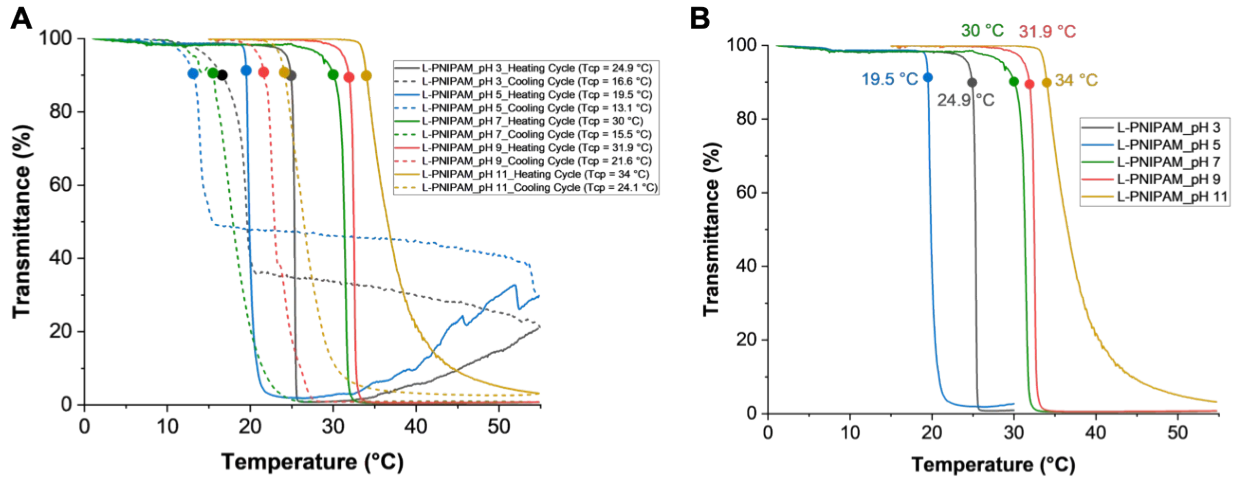

Figure S6. (**A**) Cloud point temperature profiles of linear P(NIPAM$_{96}$-*co*-FluA$_4$) at varying pH (pH = 3, 5, 7.4, 9, 11) at 5 mg/mL with heating/cooling cycles and (**B**) without cooling cycles.

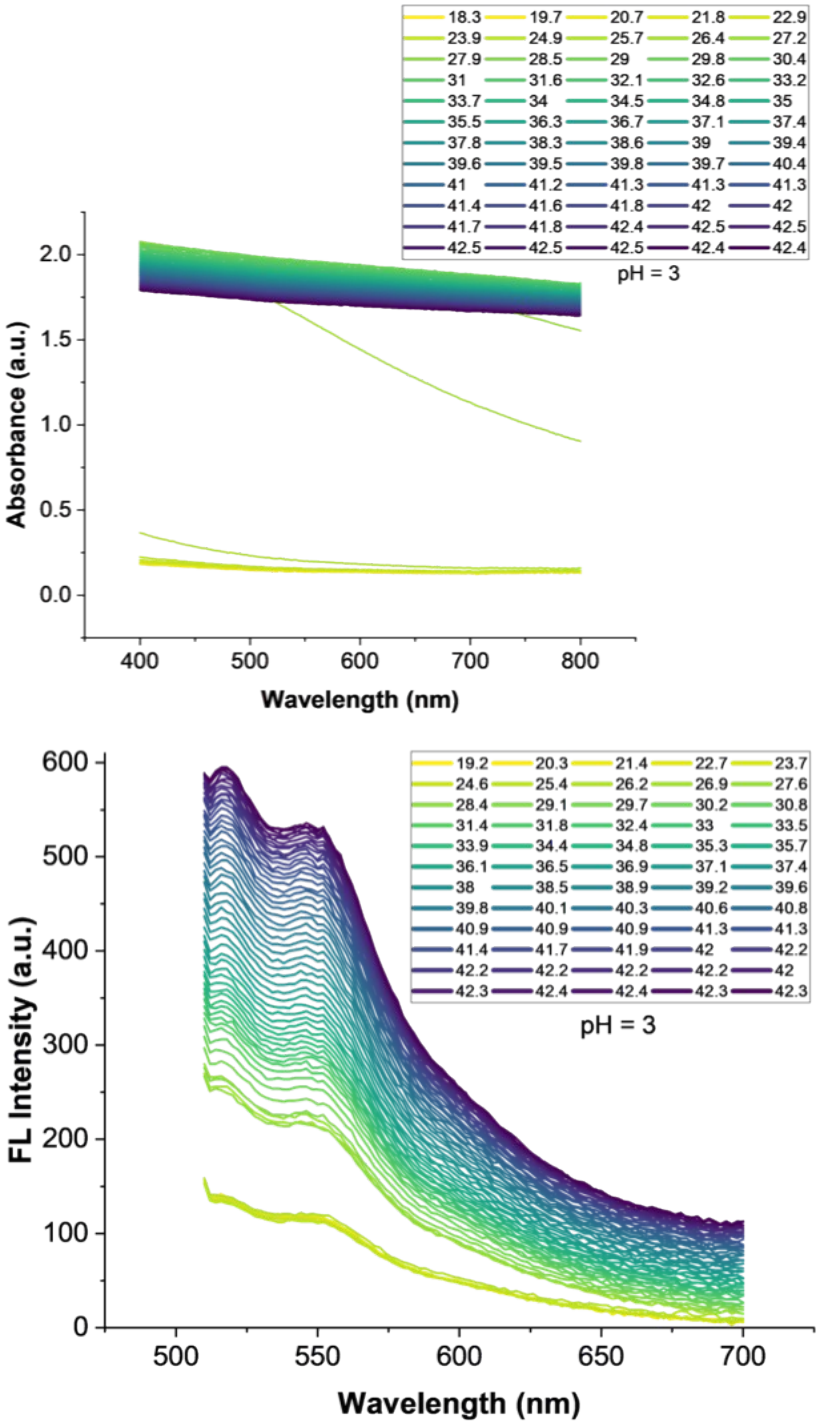

Figure S7. Temperature-dependent absorbance (top) and fluorescence emission spectrum (λ_{ex} = 490 nm) (bottom) of linear P(NIPAM$_{96}$-*co*-FluA$_4$) at pH=3 at 5 mg/mL.

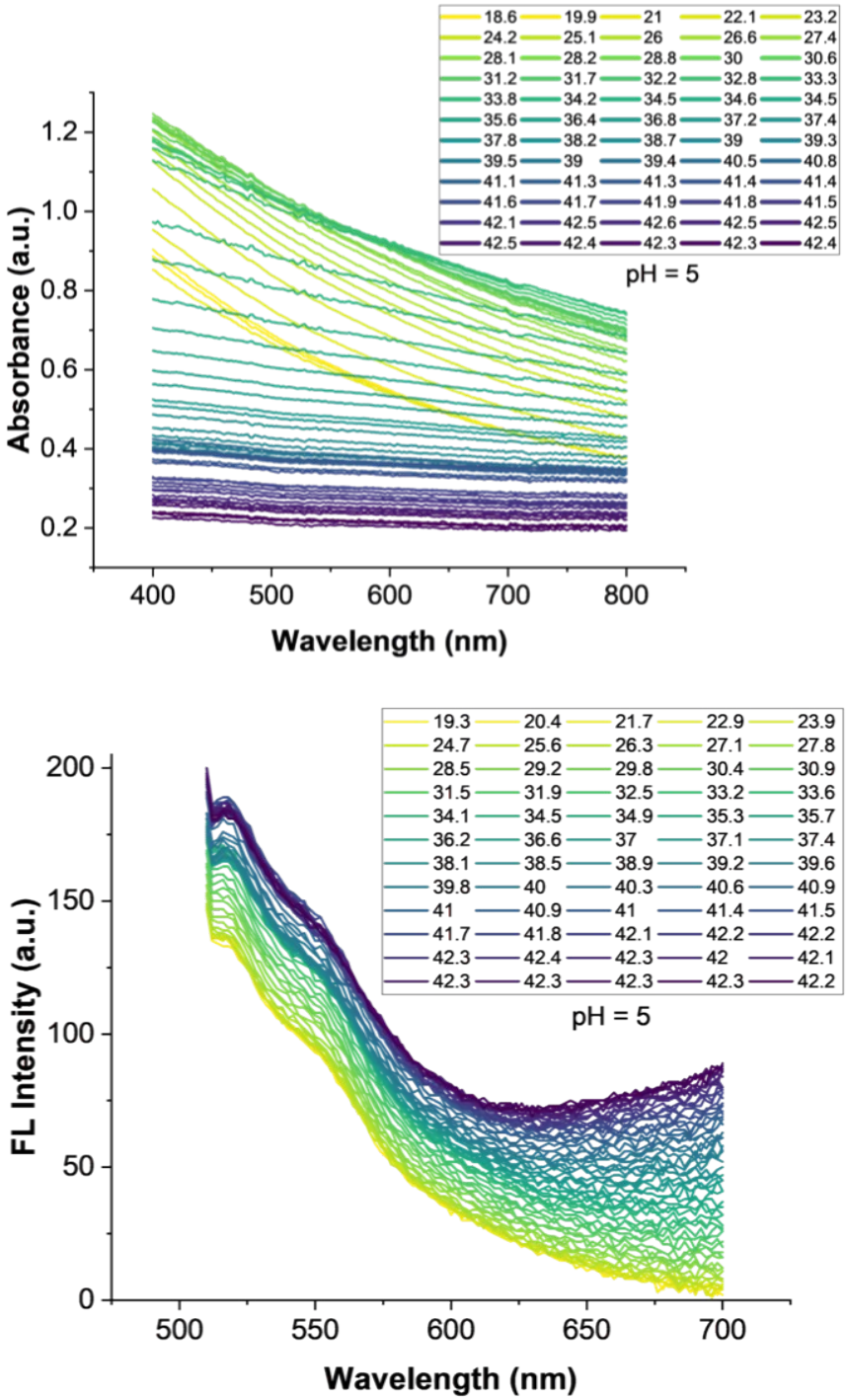

Figure S8. Temperature-dependent absorbance (top) and fluorescence emission spectrum (λ_{ex} = 490 nm) (bottom) of linear P(NIPAM$_{96}$-*co*-FluA$_4$) at pH=5 at 5 mg/mL.

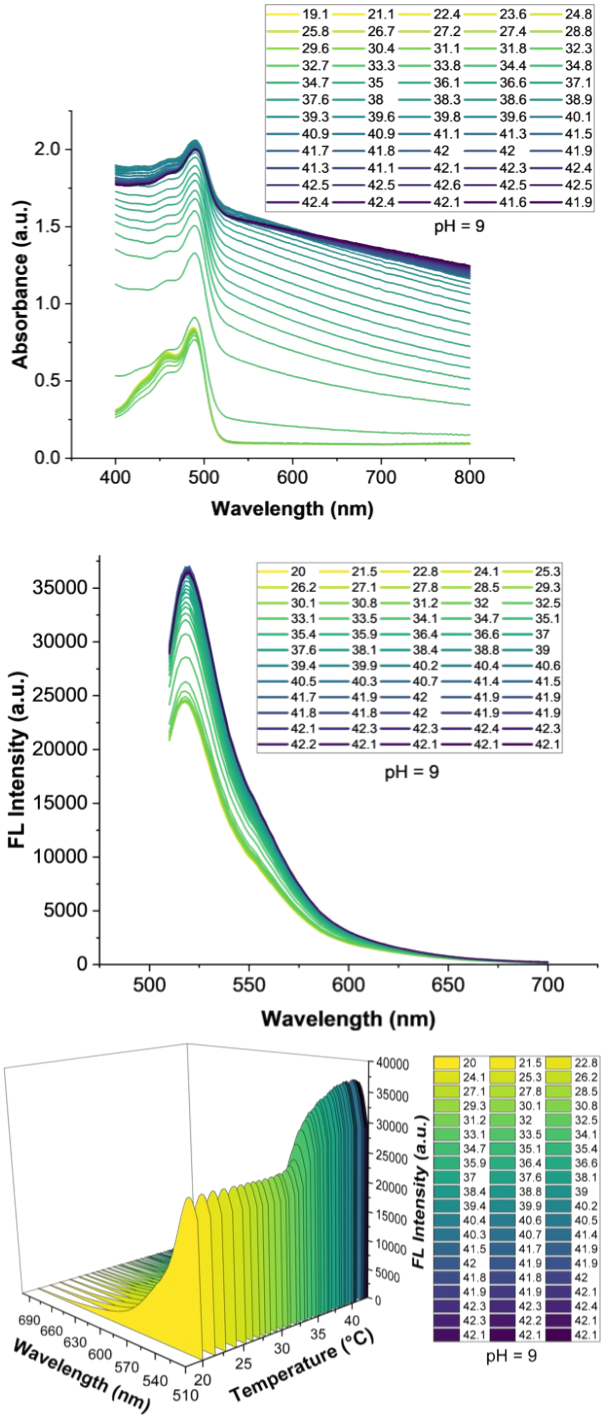

Figure S9. Temperature-dependent absorbance (top), fluorescence emission spectrum (middle) (λ_{ex} = 490 nm), 3D representation of fluorescence emission spectrum (λ_{ex} = 490 nm) (bottom) of linear P(NIPAM$_{96}$-co-FluA$_4$) at pH=9 at 5 mg/mL.

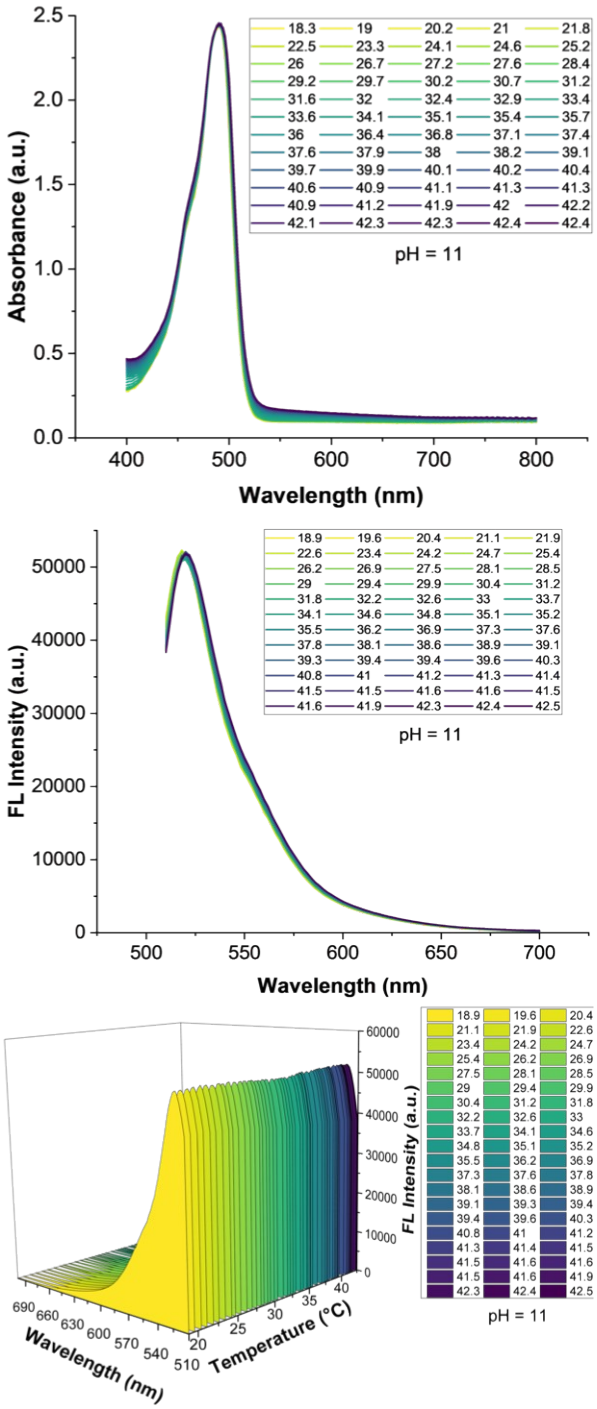

Figure S10. Temperature-dependent absorbance (top), fluorescence emission spectrum (λ_{ex} = 490 nm) (middle), 3D representation of fluorescence emission spectrum (λ_{ex} = 490 nm) (bottom) of linear P(NIPAM$_{96}$-*co*-FluA$_4$) at pH=11 at 5 mg/mL.

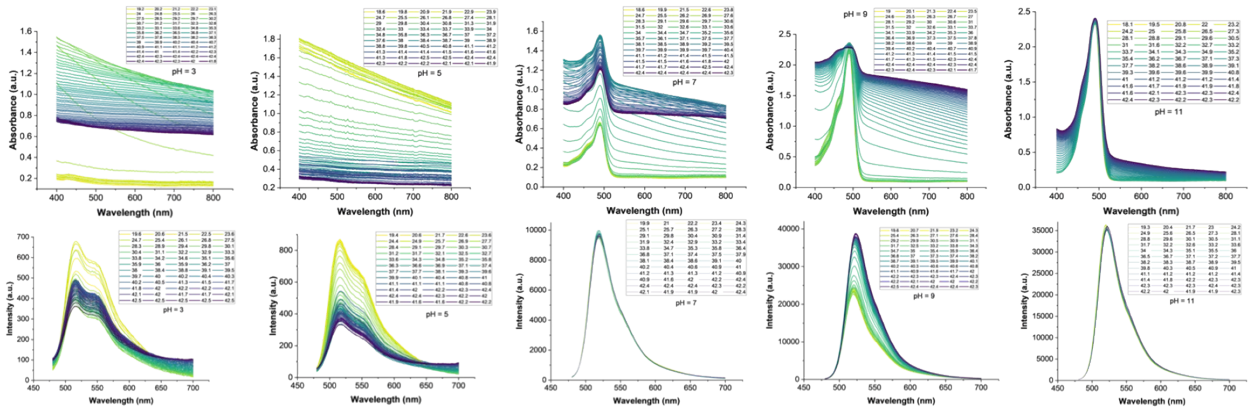

Figure S11. Temperature-dependent absorbance and fluorescence of linear P(NIPAM$_{96}$-*co*-FluA$_4$) at varying pH at 5 mg/mL when excited at 450 nm (λ_{ex}) to get the full fluorescence spectrum.

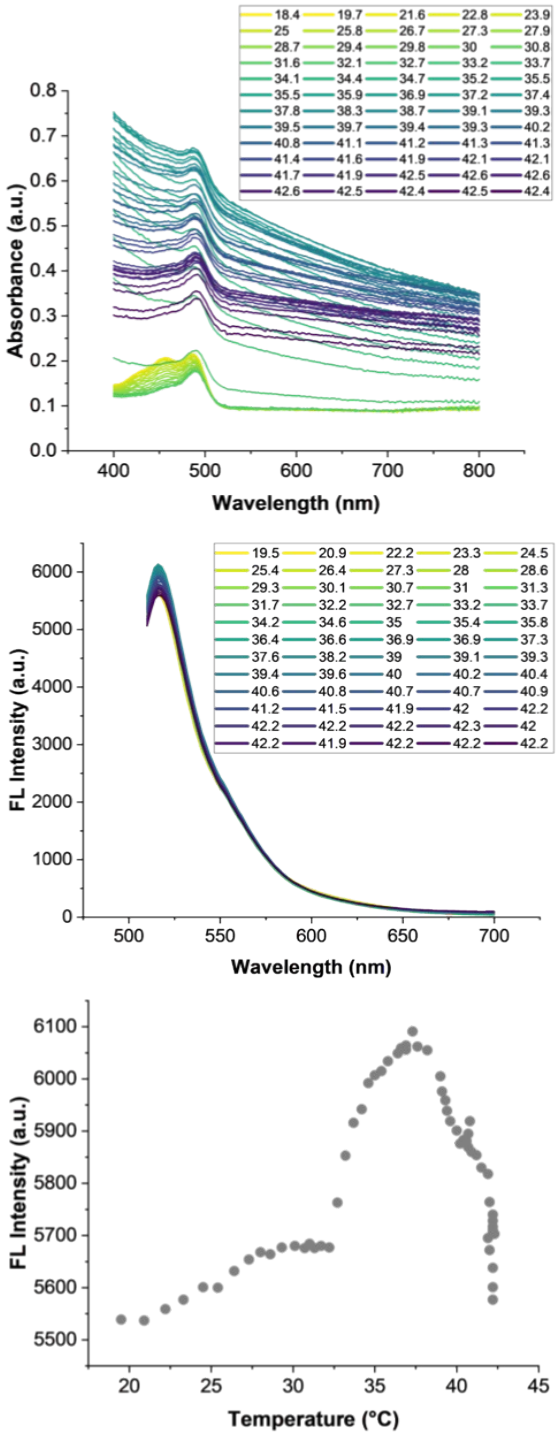

Figure S12. Temperature-dependent absorbance (top), fluorescence emission spectrum (λ_{ex} = 490 nm) (middle), and fluorescence intensity profile obtained from the corresponding peak maxima in the fluorescence emission (λ_{em} = 518 nm) spectrum (bottom) of linear P(NIPAM$_{96}$-*co*-FluA$_4$) in PBS (pH=7.4) at 1 mg/mL.

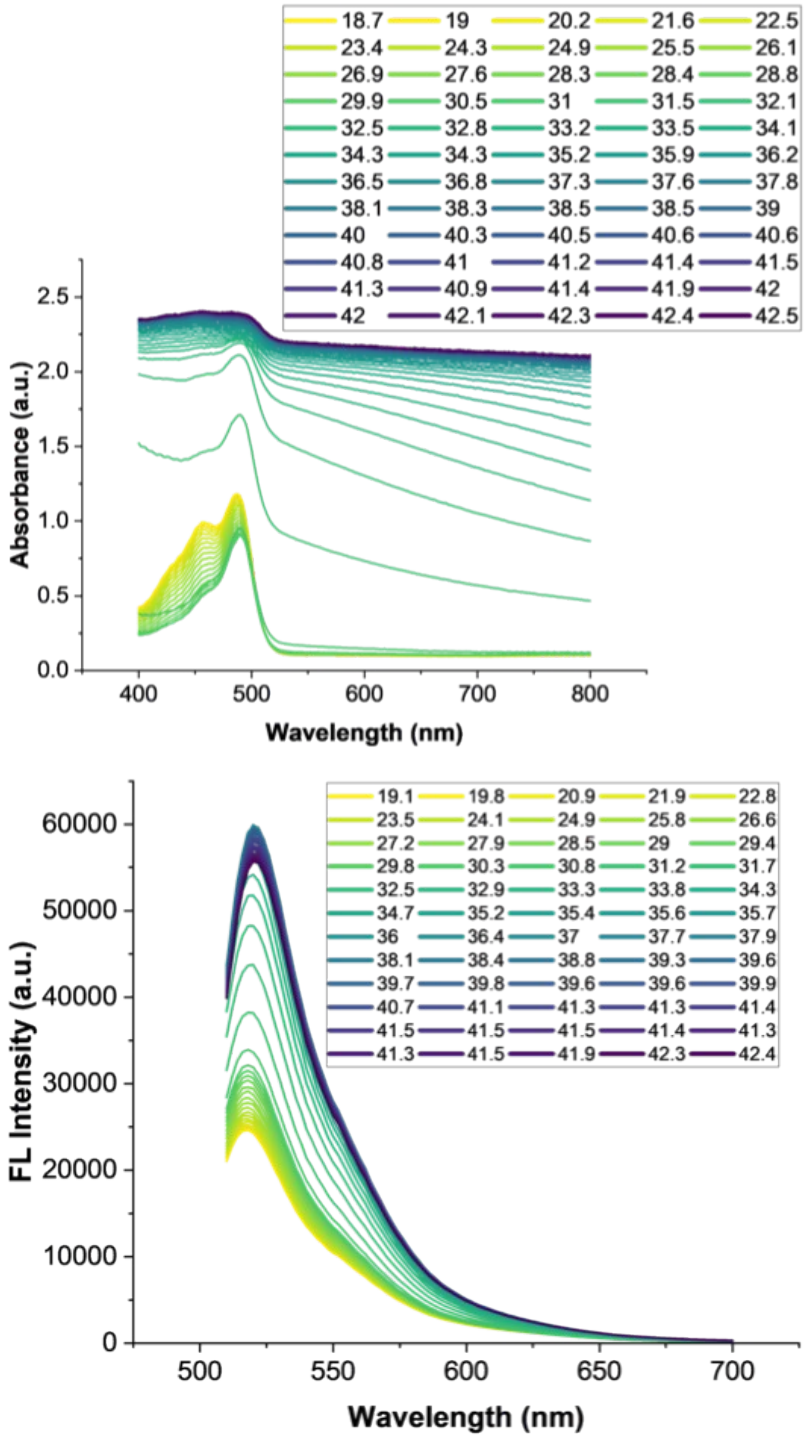

Figure S13. Temperature-dependent absorbance (top) and fluorescence emission spectrum (λ_{ex} = 490 nm) (bottom) of linear P(NIPAM$_{96}$-*co*-FluA$_4$) in PBS (pH=7.4) at 10 mg/mL.

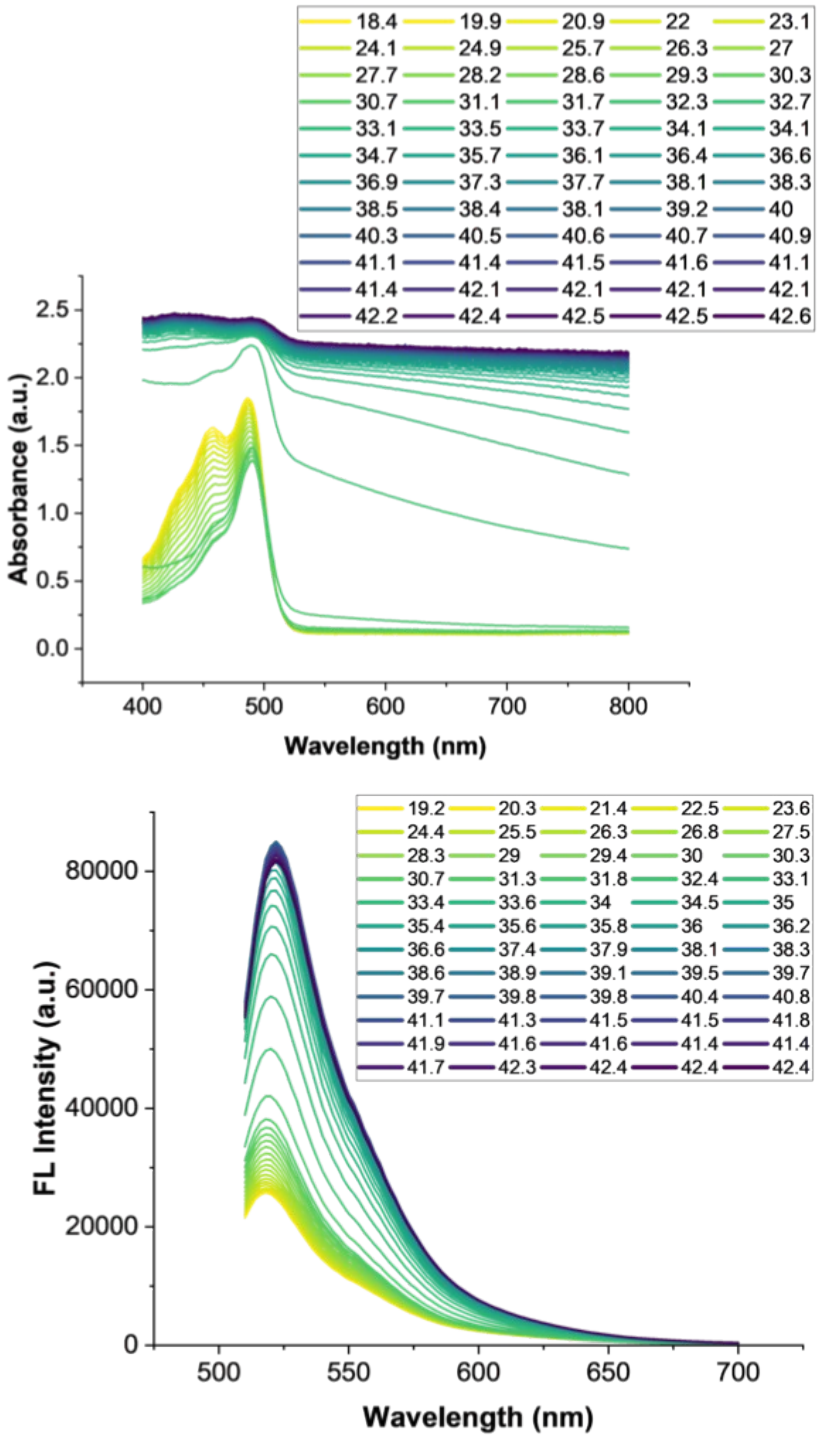

Figure S14. Temperature-dependent absorbance (top) and fluorescence emission spectrum (λ_{ex} = 490 nm) (bottom) of linear P(NIPAM$_{96}$-*co*-FluA$_4$) in PBS (pH=7.4) at 20 mg/mL.

3. Ethylene Glycol Methacrylate-based Linear Thermoresponsive Fluorescent Polymers

3.1. P(OEGMA$_{500}$-*co*-DEGMA-*co*-FluA) (Feed ratio = 5:90:5)

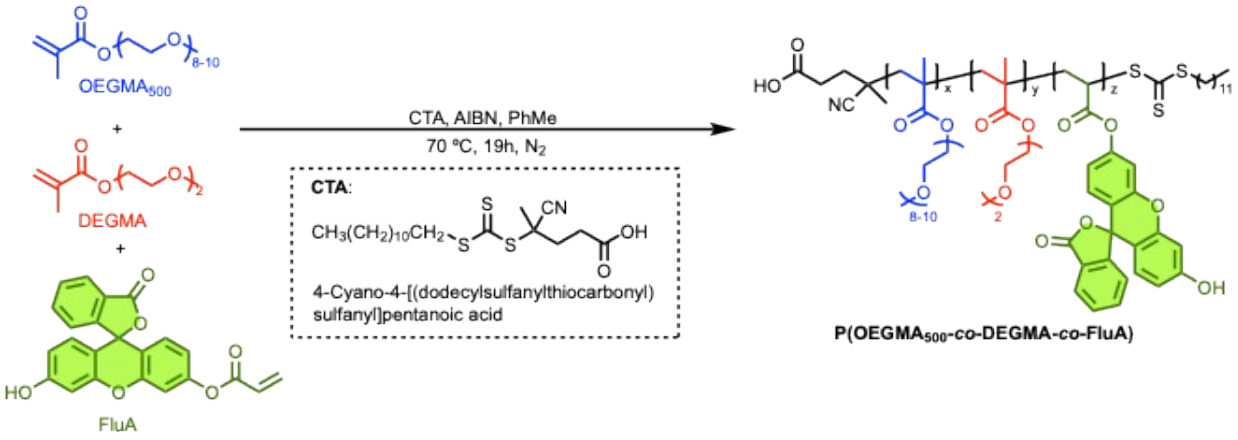

Scheme S3. Synthesis of P(OEGMA-*co*-DEGMA-*co*-FluA) via RAFT polymerization.

Purified OEGMA$_{500}$ (154.0 mg, 0.31 mmol), purified DEGMA (1.200 g, 5.42 mmol), FluA (116.1 mg, 0.30 mmol)), CTDPA (5.9mg, 0.014 mmol), and AIBN (2.7 mg, 0.016 mmol) were dissolved in toluene (2 mL) in a 25mL Schlenk flask equipped with a Teflon-coated stir bar. The reaction mixture was deoxygenated by purging and sparging with N_2 for 10 min. After sparging, the Schlenk flask with the reaction mixture was heated at 70 °C for 19 hours. The obtained terpolymer was purified by precipitating in hexanes three times and then dried under vacuum for further characterization, with an isolated yield of 1.464 g. Actual Composition = 6.5:82.3:11.2 by ^{1}H NMR Spectroscopy; SEC-MALS (DMF) characterization: M_n = 113 kDa, Đ = 2.7.

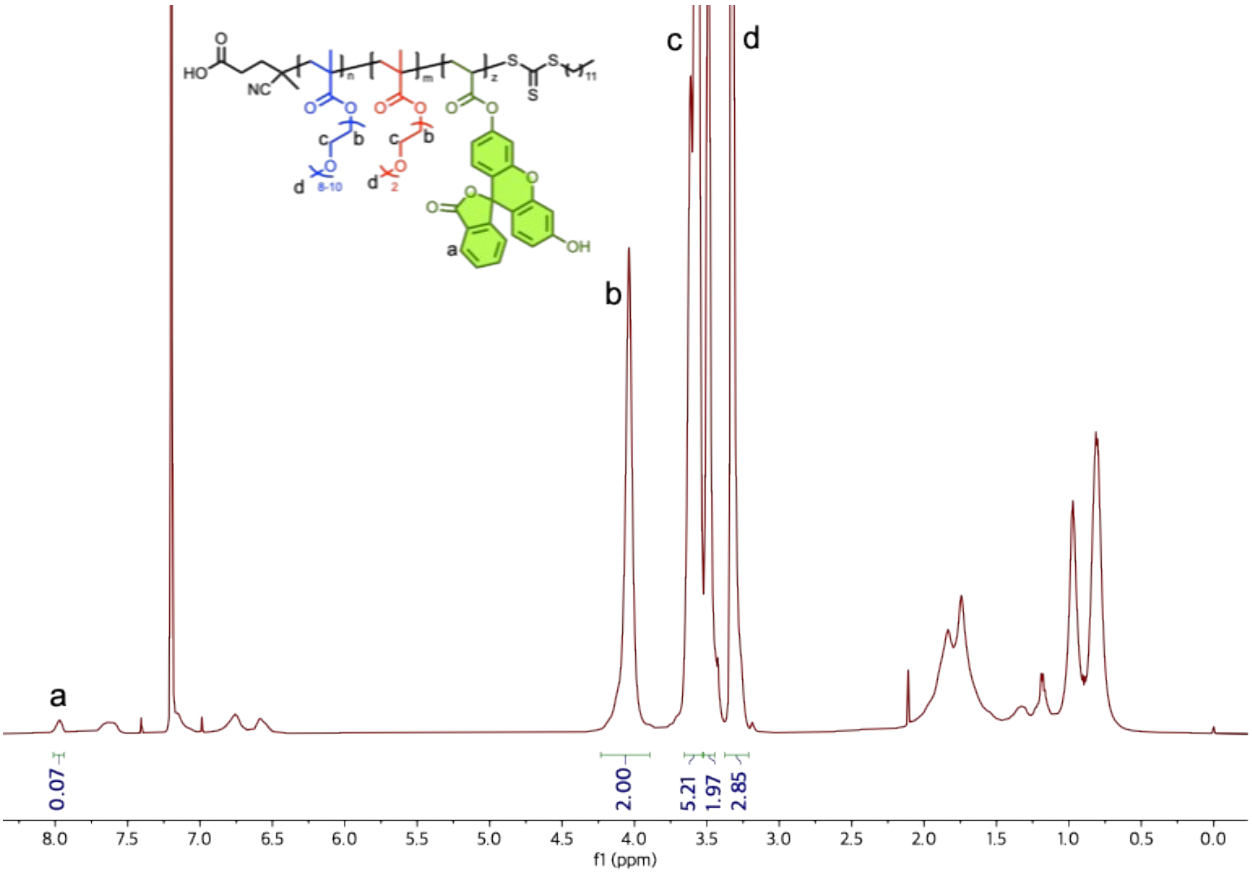

Figure S15. ^{1}H NMR spectrum of P(OEGMA$_{6.5}$-*co*-DEGMA$_{82.3}$-*co*-FluA$_{11.2}$) synthesized via conventional RAFT polymerization in $CDCl_3$.

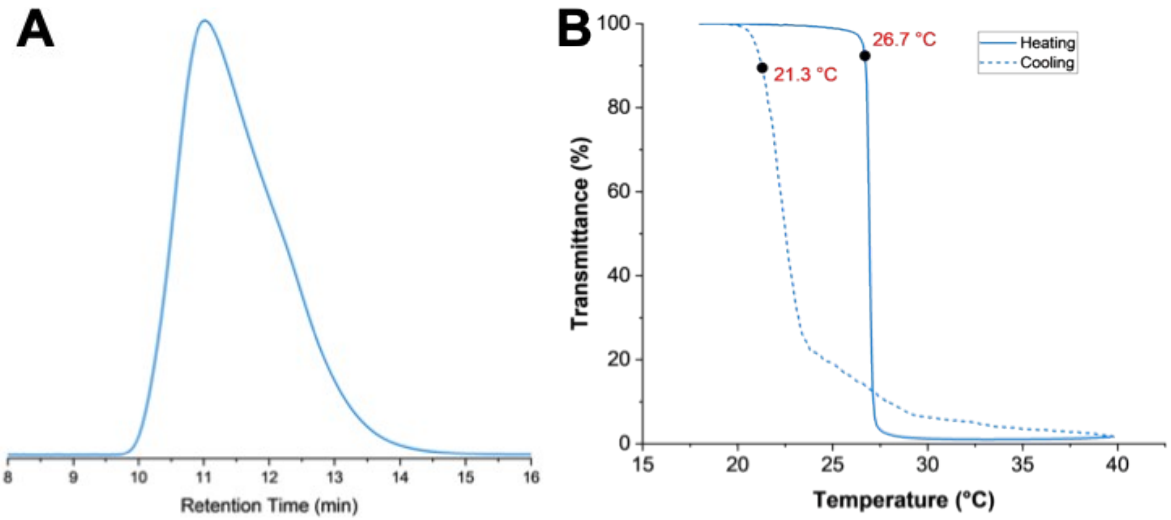

Figure S16. **(A)** SEC-MALS (DMF) trace, **(B)** absorbance and fluorescence spectra at 0.1 mg/mL, and **(C)** cloud point temperature profile at 10 mg/mL of linear P(OEGMA$_{6.5}$-*co*-DEGMA$_{82.3}$-*co*-FluA$_{11.2}$) synthesized via conventional RAFT polymerization.

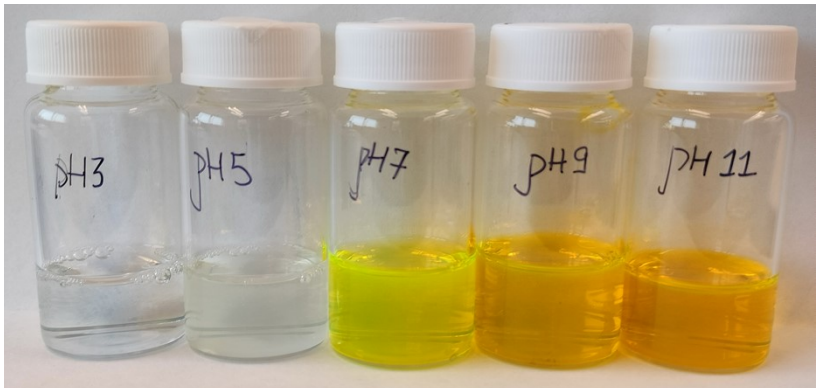

Figure S17. Visual comparison of linear P(OEGMA$_{6.5}$-*co*-DEGMA$_{82.3}$-*co*-FluA$_{11.2}$) solubility/behavior in solutions of varying pH (3, 5, 7.4, 9, and 11).

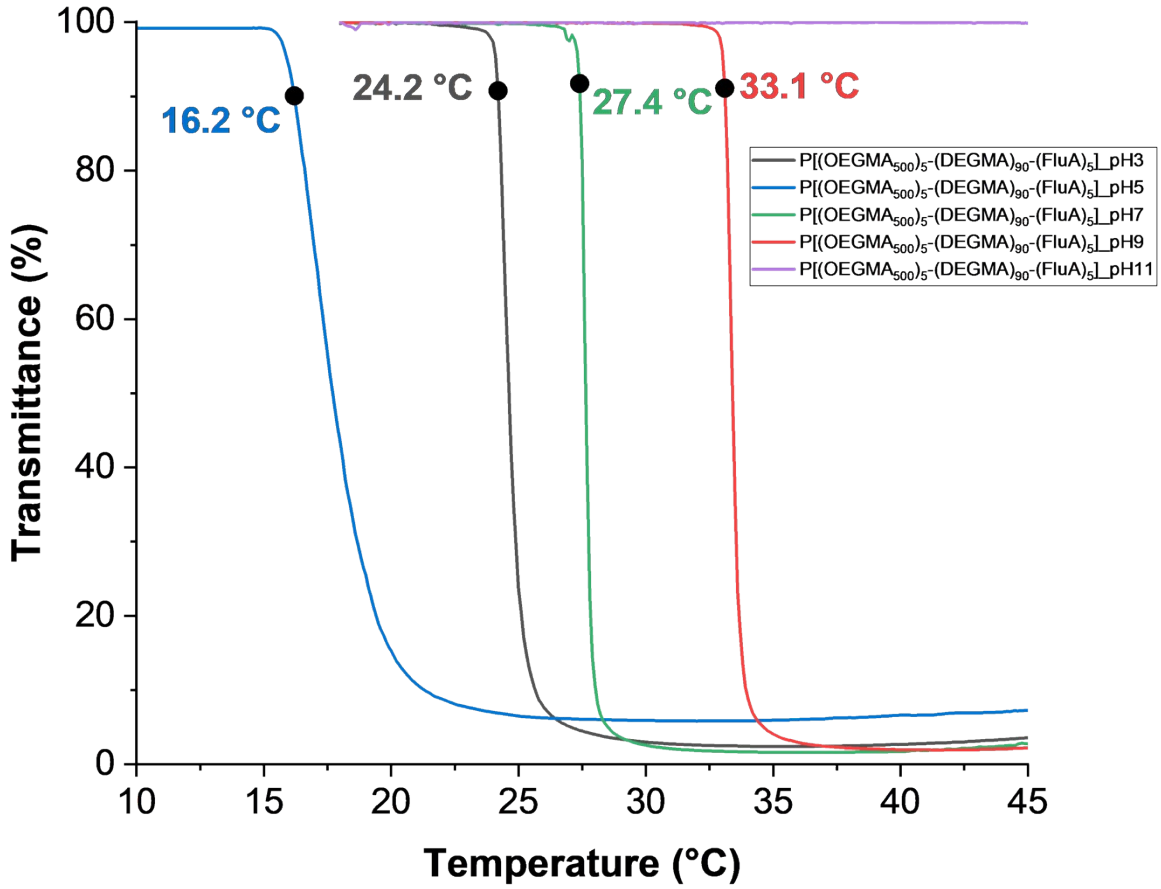

Figure S18. Cloud point temperature profiles of linear P(OEGMA$_{6.5}$-*co*-DEGMA$_{82.3}$-*co*-FluA$_{11.2}$) at varying pH (pH 3, 5, 7.4, 9 and 11) at 5 mg/mL.

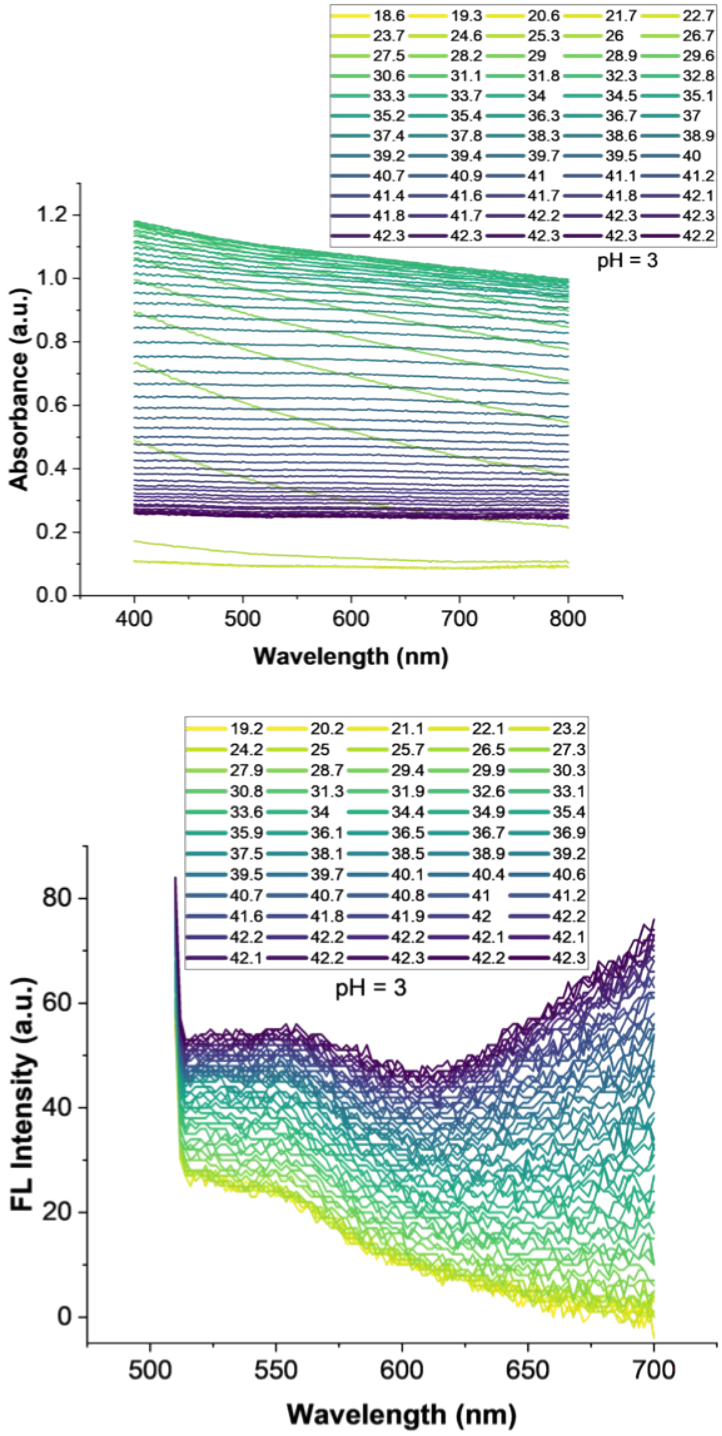

Figure S19. Temperature-dependent absorbance (top) and fluorescence emission spectrum (λ_{ex} = 490 nm) (bottom) of linear P(OEGMA$_{6.5}$-*co*-DEGMA$_{82.3}$-*co*-FluA$_{11.2}$) at pH=3 at 5 mg/mL.

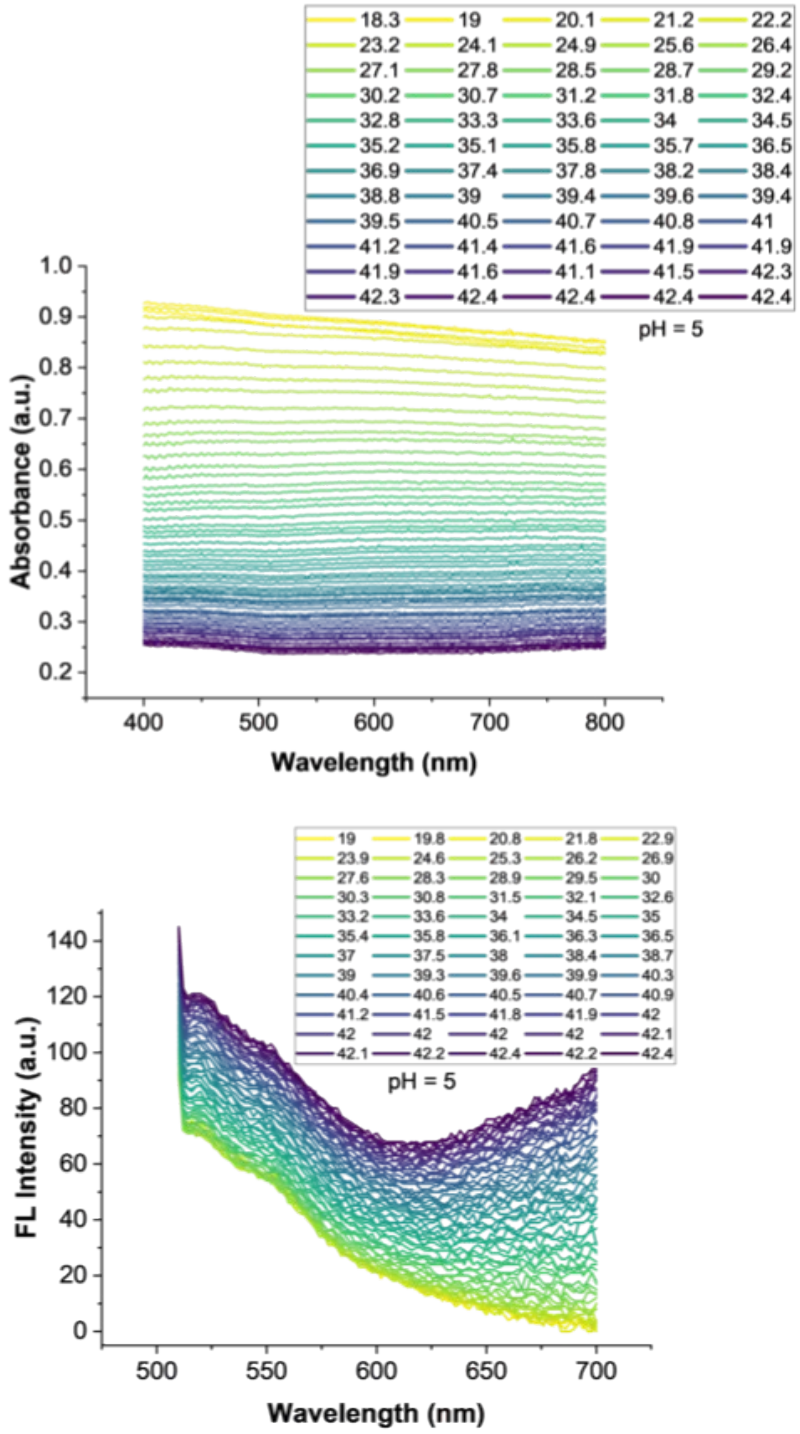

Figure S20. Temperature-dependent absorbance (top) and fluorescence emission spectrum (λ_{ex} = 490 nm) (bottom) of linear P(OEGMA$_{6.5}$-*co*-DEGMA$_{82.3}$-*co*-FluA$_{11.2}$) at pH=5 at 5 mg/mL.

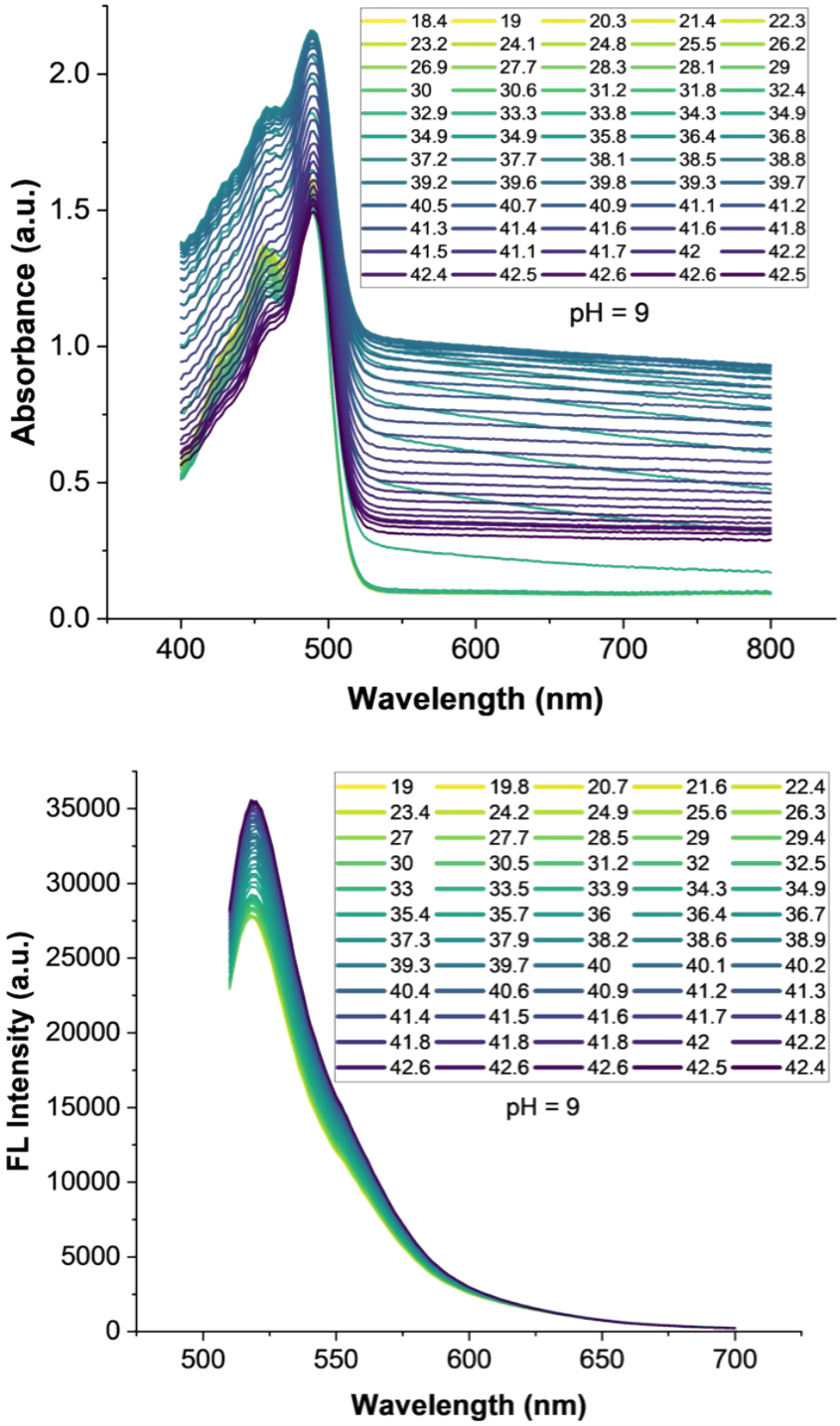

Figure S21. Temperature-dependent absorbance (top) and fluorescence emission spectrum (λ_{ex} = 490 nm) (bottom) of linear P(OEGMA$_{6.5}$-*co*-DEGMA$_{82.3}$-*co*-FluA$_{11.2}$) at pH=9 at 5 mg/mL.

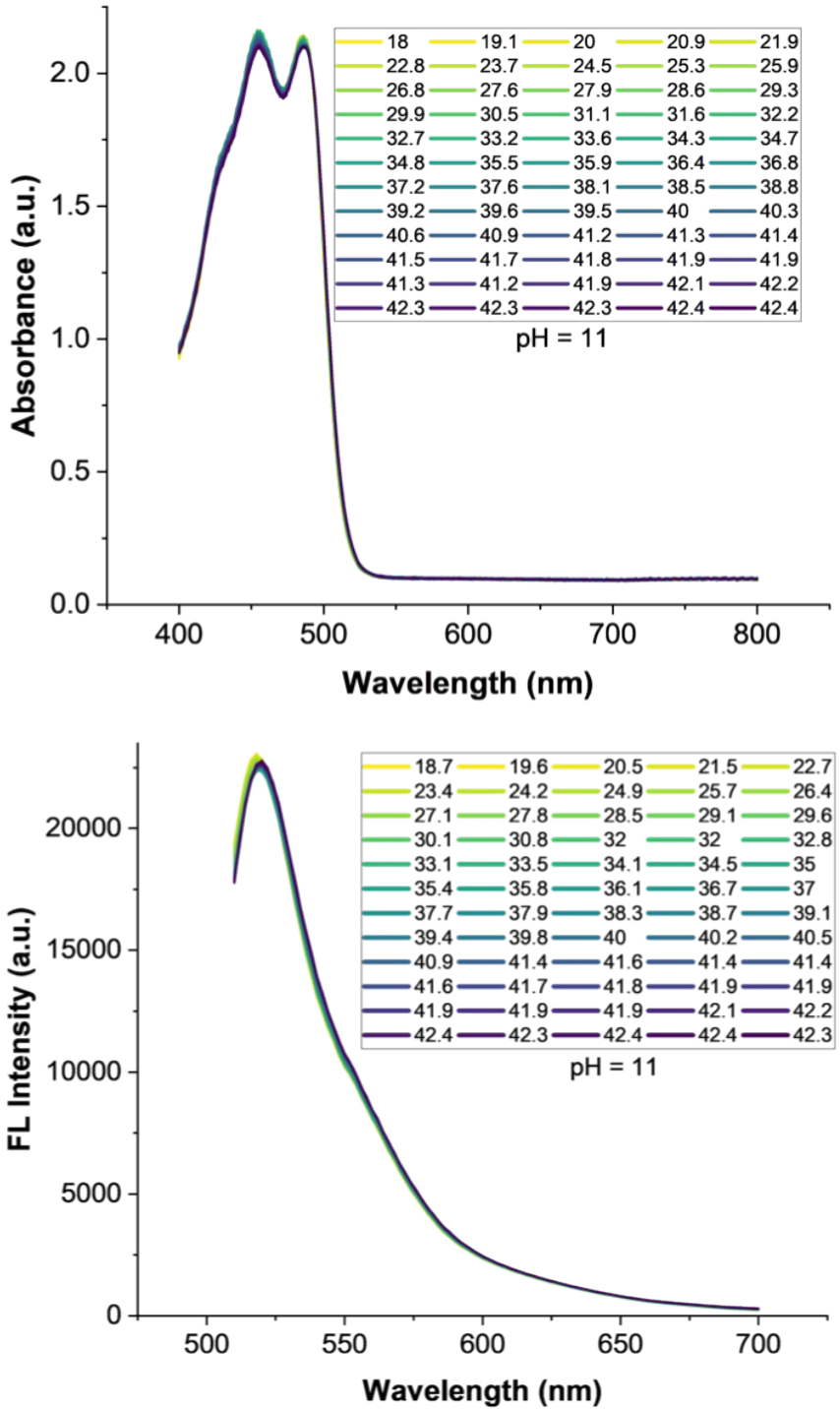

Figure S22. Temperature-dependent absorbance (top) and fluorescence emission spectrum (λ_{ex} = 490 nm) (bottom) of linear P(OEGMA$_{6.5}$-*co*-DEGMA$_{82.3}$-*co*-FluA$_{11.2}$) at pH=11 at 5 mg/mL.

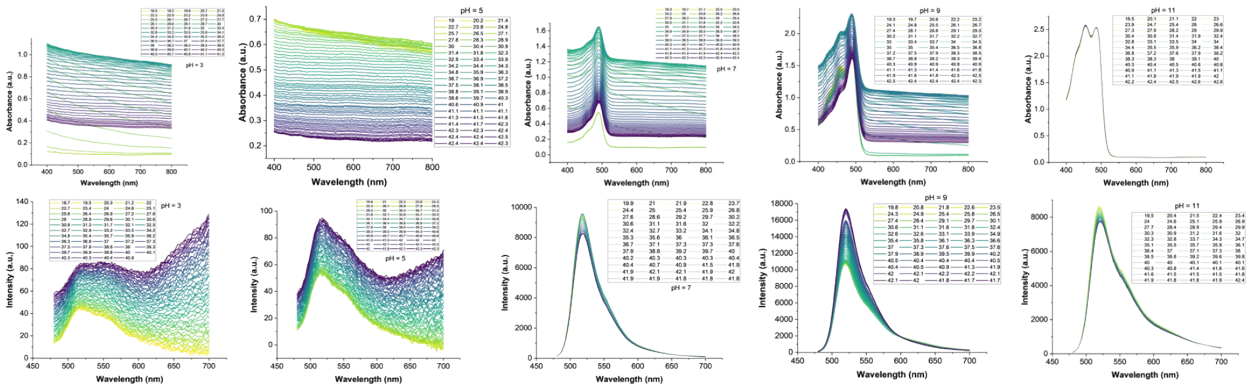

Figure S23. Temperature-dependent absorbance and fluorescence emission spectrum of linear P(OEGMA$_{6.5}$-*co*-DEGMA$_{82.3}$-*co*-FluA$_{11.2}$) at varying pH at 5 mg/mL when excited at 450 nm (λ_{ex}) to get the full fluorescence spectrum.

3.2. P(OEGMA$_{500}$-*co*-DEGMA-*co*-FluA) (Feed ratio = 10:89:1)

Purified OEGMA$_{500}$ (0.28 mL, 0.61 mmol), purified DEGMA (1 mL, 5.42 mmol), FluA (23.5 mg, 0.06 mmol), CTDPA (4.9 mg, 0.01 mmol), and AIBN (2 mg, 0.01 mmol) were dissolved in toluene (2 mL) in a 25 mL Schlenk flask equipped with a Teflon-coated stir bar. The reaction mixture was deoxygenated by purging and sparging with N_2 for 10 min. After sparging, the Schlenk flask with the reaction mixture was heated at 70 °C for 19 hours. The obtained terpolymer was purified by precipitating in hexanes three times and then dried under vacuum for further characterization, with an isolated yield of 1.16 g. Actual Composition = 16.3:80.8:2.9 ~ 16:81:3 by ^{1}H NMR Spectroscopy; SEC-MALS (DMF) characterization: M_n = 198.3 kDa, Đ = 2.02.

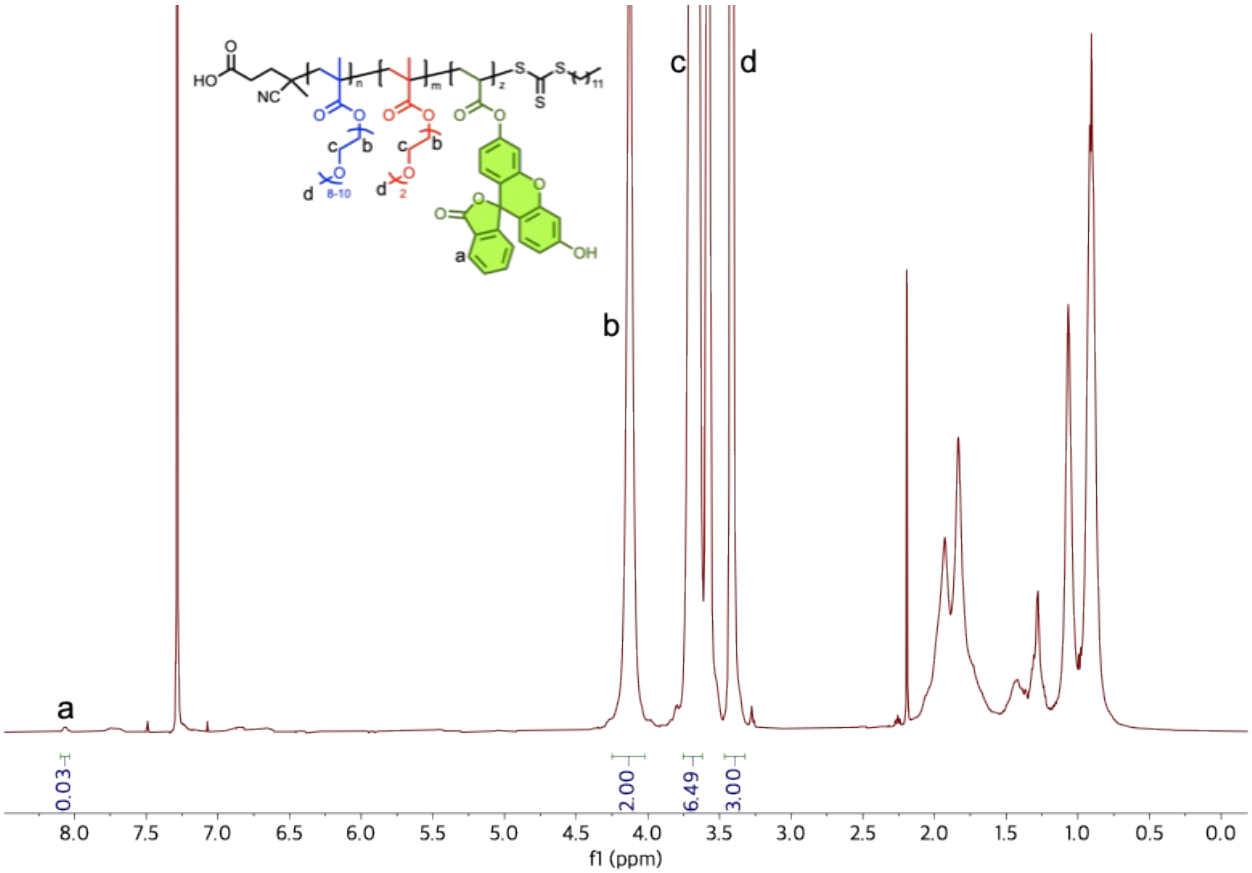

Figure S24. ^{1}H NMR spectrum of P(OEGMA$_{16}$-*co*-DEGMA$_{81}$-*co*-FluA$_{3}$) synthesized via conventional RAFT polymerization in $CDCl_3$.

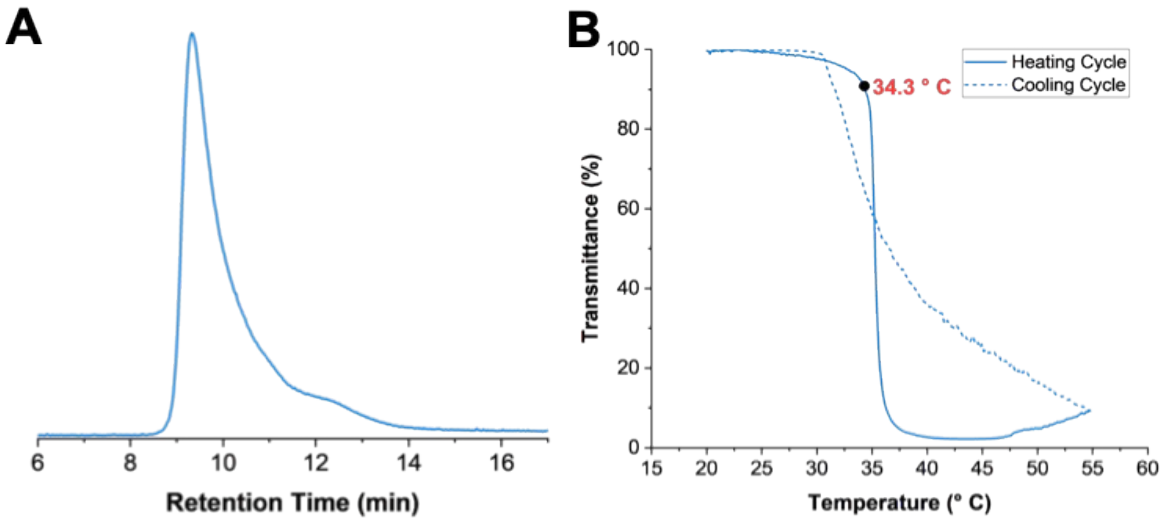

Figure S25. **(A)** SEC-MALS (DMF) trace and **(B)** cloud point temperature profile at 10 mg/mL of linear P(OEGMA$_{16}$-*co*-DEGMA$_{81}$-*co*-FluA$_3$) synthesized via conventional RAFT polymerization.

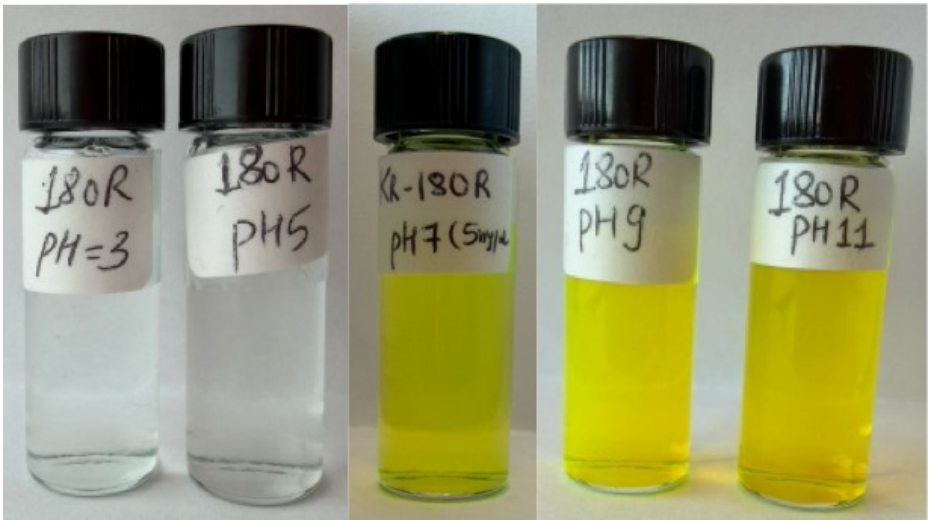

Figure S26. Visual comparison of linear P(OEGMA$_{16}$-*co*-DEGMA$_{81}$-*co*-FluA$_3$) solubility/behavior in solutions of varying pH (3, 5, 7.4, 9, and 11).

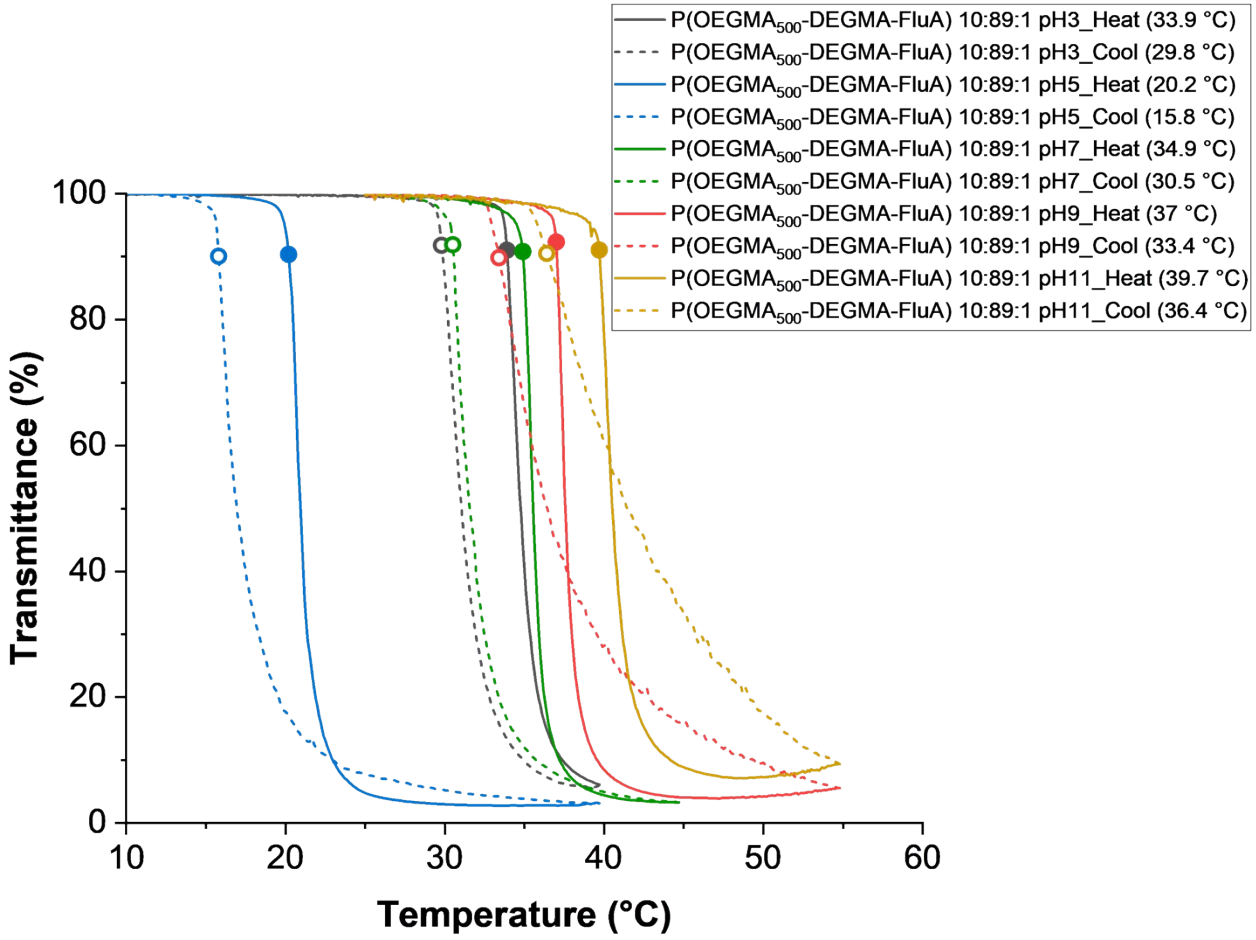

Figure S27. Cloud point temperature profiles of linear P(OEGMA$_{16}$-*co*-DEGMA$_{81}$-*co*-FluA$_3$) at varying pH (pH 3, 5, 7.4, 9, 11) at 5 mg/mL with heating/cooling cycles.

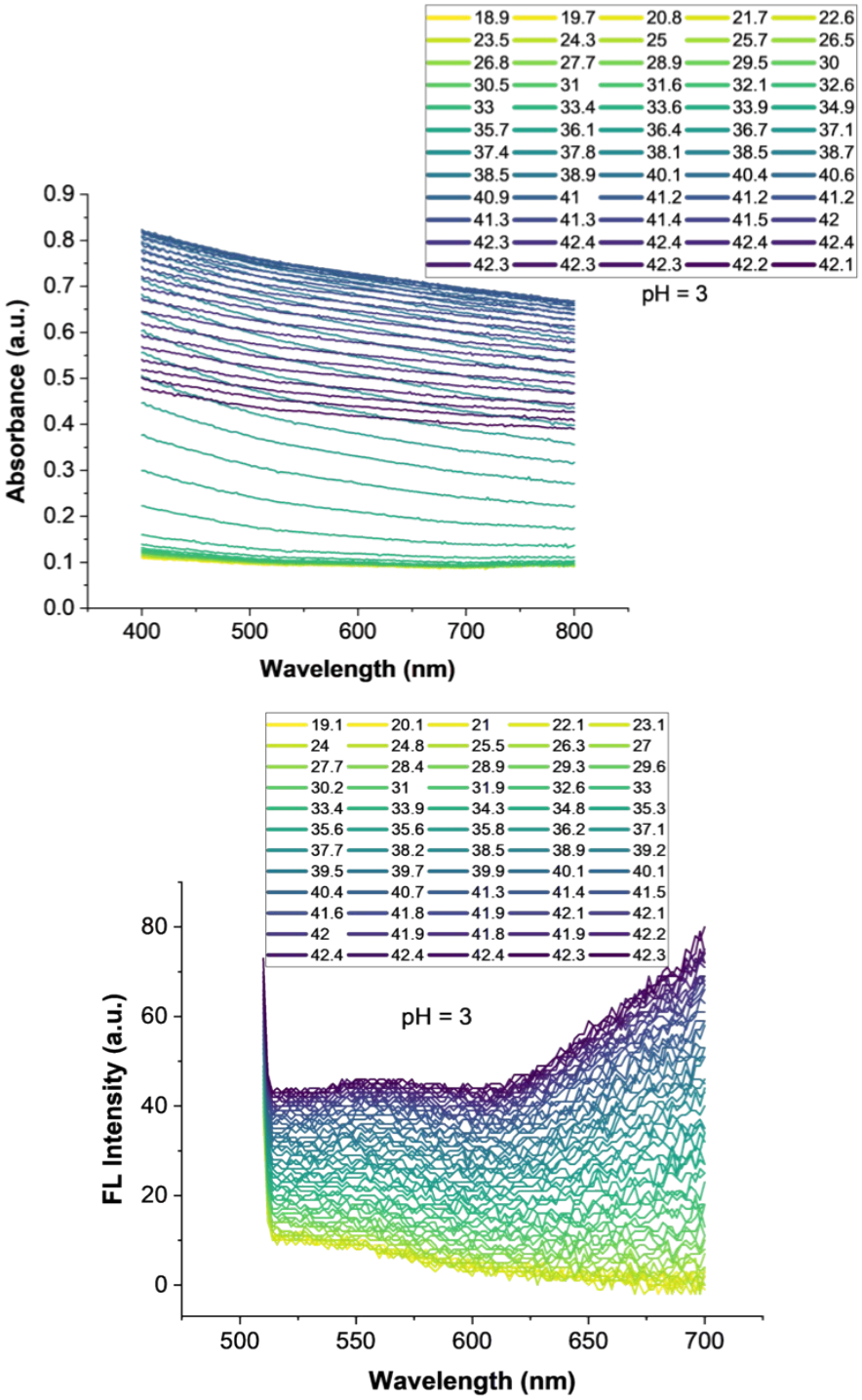

Figure S28. Temperature-dependent absorbance (top) and fluorescence emission spectrum (λ_{ex} = 490 nm) (bottom) of linear P(OEGMA$_{16}$-*co*-DEGMA$_{81}$-*co*-FluA$_3$) at pH=3 at 5 mg/mL.

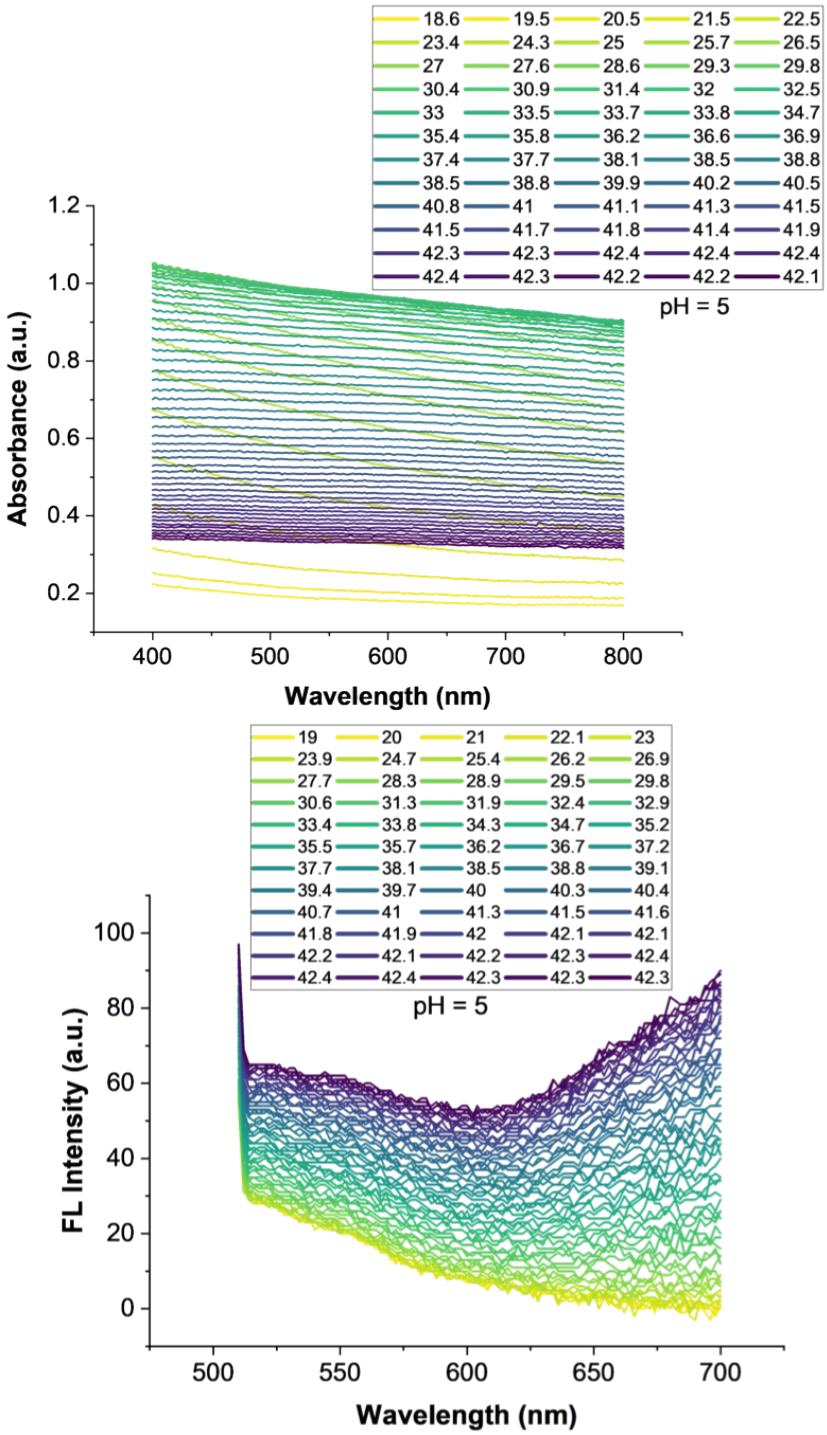

Figure S29. Temperature-dependent absorbance (top) and fluorescence emission spectrum (λ_{ex} = 490 nm) (bottom) of linear P(OEGMA$_{16}$-*co*-DEGMA$_{81}$-*co*-FluA$_3$) at pH=5 at 5 mg/mL.

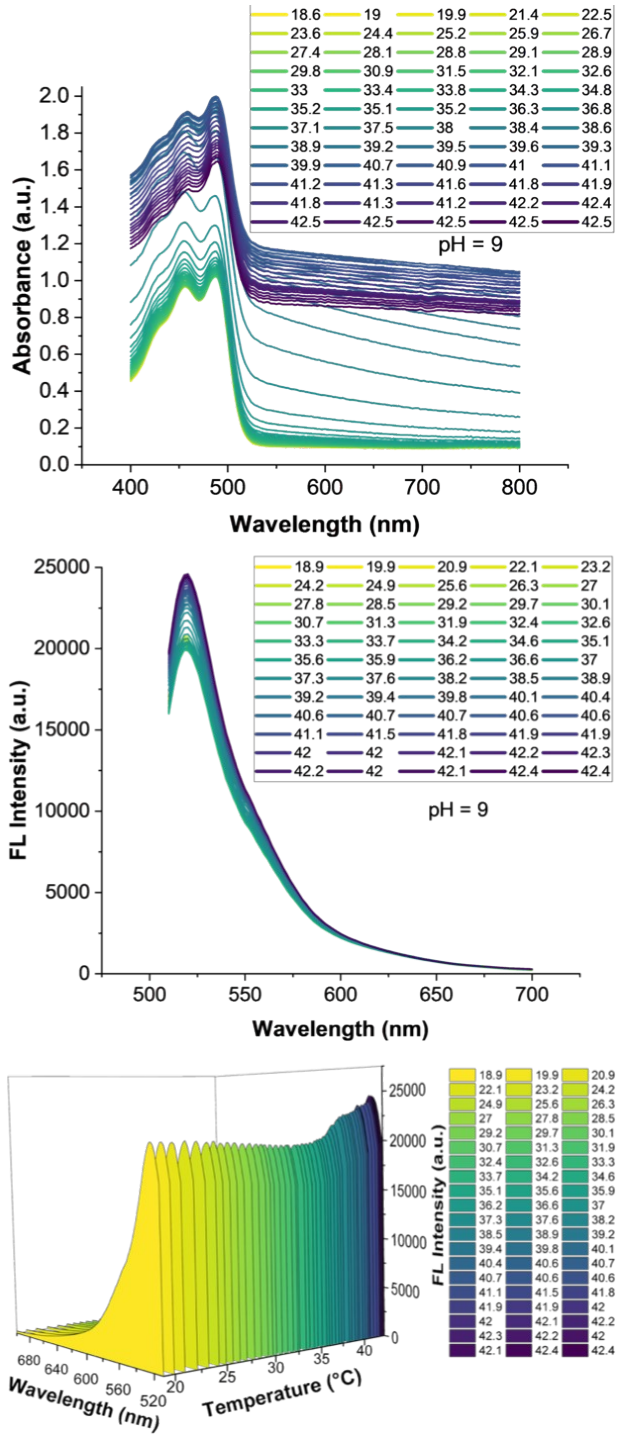

Figure S30. Temperature-dependent absorbance (top), fluorescence emission spectrum (middle), and 3D representation for fluorescence emission spectrum (λ_{ex} = 490 nm) (bottom) of linear P(OEGMA$_{16}$-*co*-DEGMA$_{81}$-*co*-FluA$_3$) at pH=9 at 5 mg/mL.

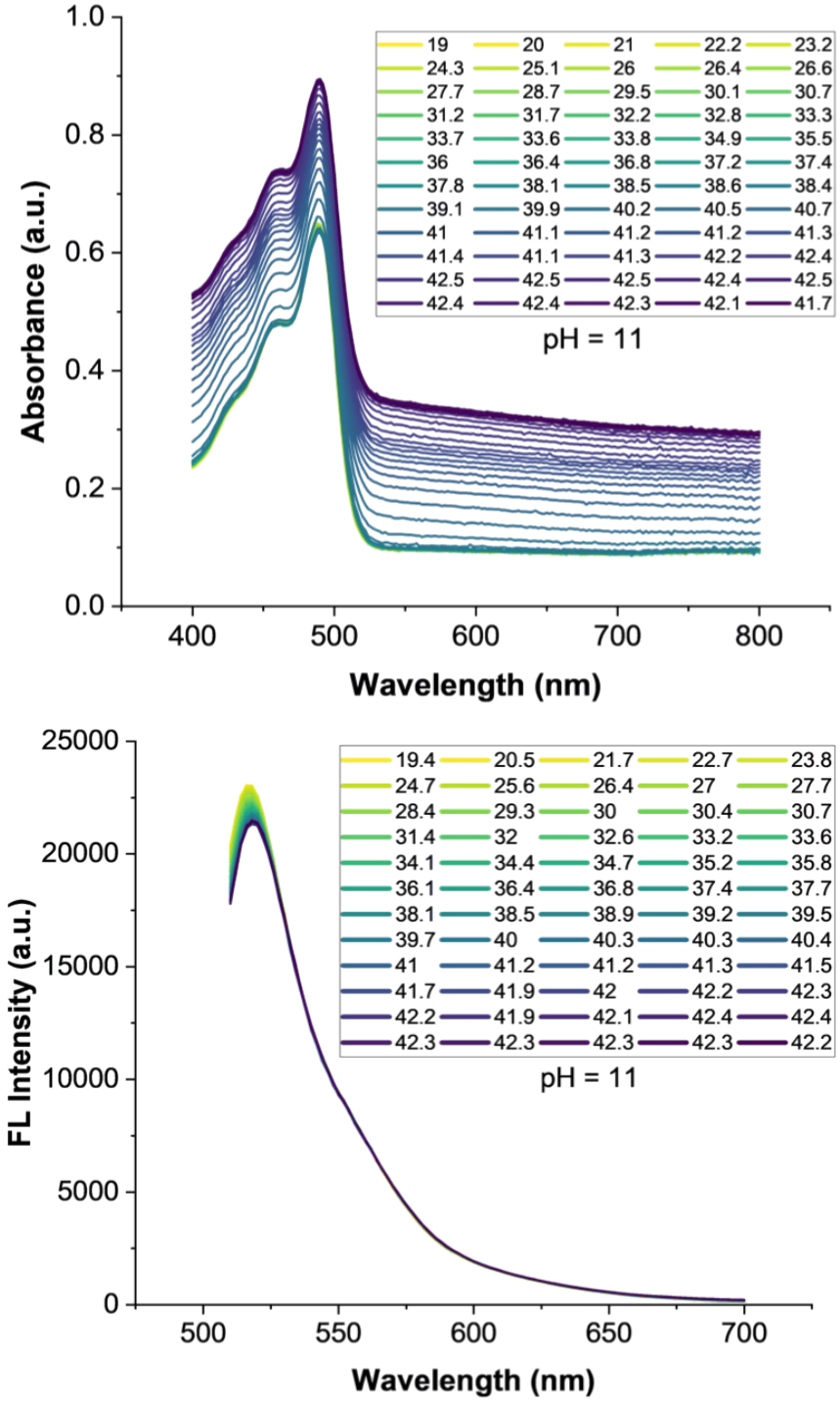

Figure S31. Temperature-dependent absorbance (top) and fluorescence emission spectrum (λ_{ex} = 490 nm) (bottom) of linear P(OEGMA$_{16}$-*co*-DEGMA$_{81}$-*co*-FluA$_3$) at pH=11 at 5 mg/mL.

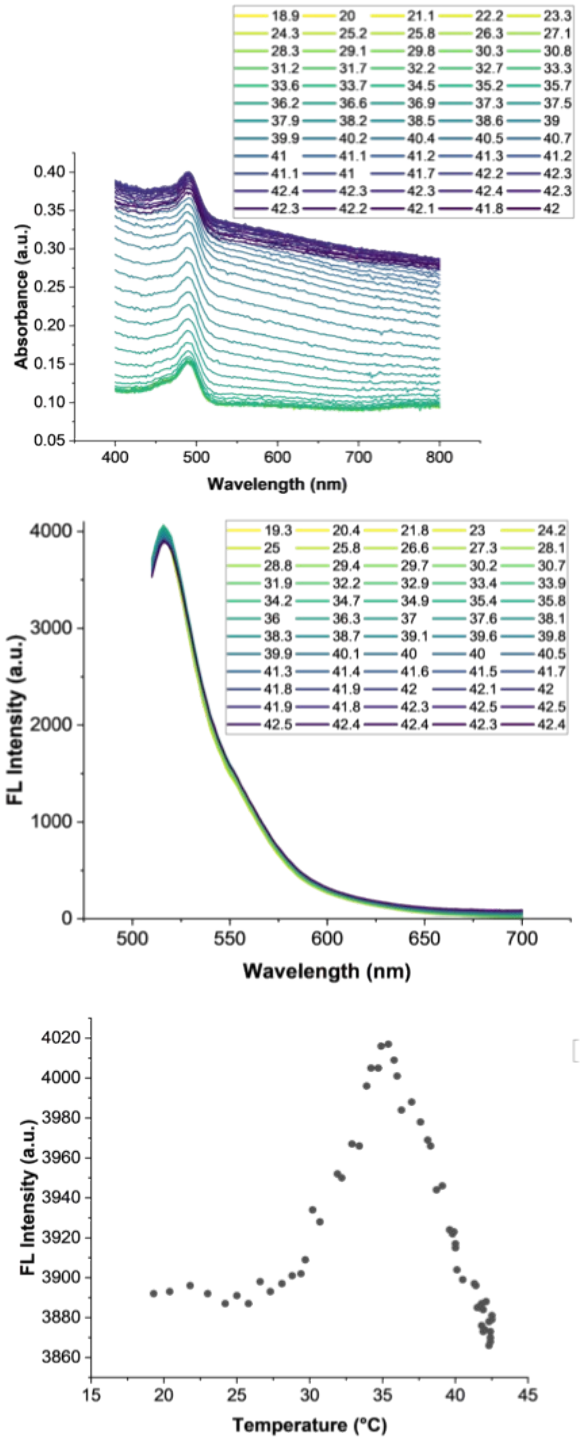

Figure S32. Temperature-dependent absorbance (top) and fluorescence emission spectrum (λ_{ex} = 490 nm) (middle), and fluorescence intensity profile obtained from the corresponding peak maxima in the fluorescence emission (λ_{em} = 518 nm) spectrum (bottom) of linear P(OEGMA$_{16}$-co-DEGMA$_{81}$-co-FluA$_3$) in PBS (pH=7.4) at 1 mg/mL.

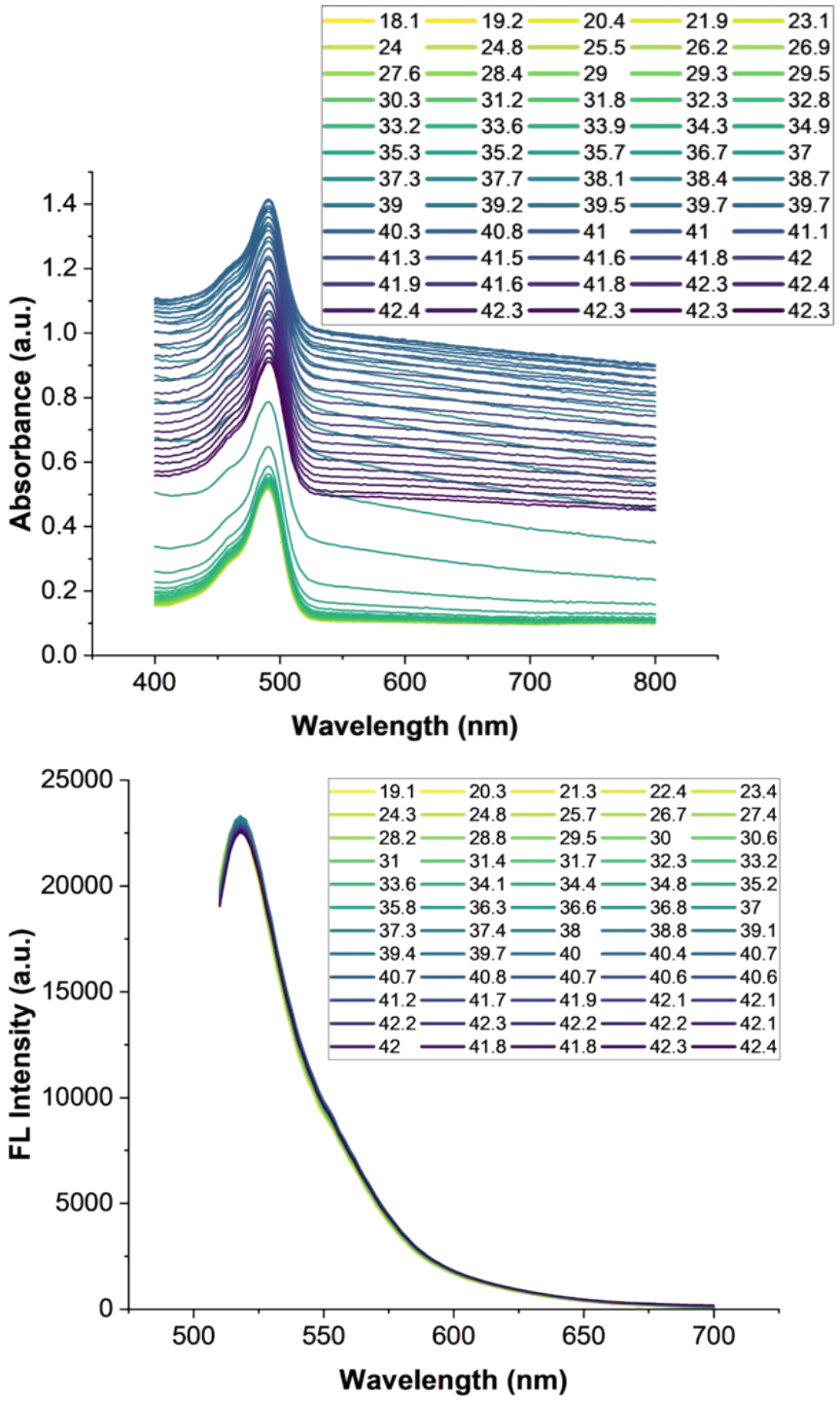

Figure S33. Temperature-dependent absorbance (top) and fluorescence emission spectrum (λ_{ex} = 490 nm) (bottom) of linear P(OEGMA$_{16}$-co-DEGMA$_{81}$-co-FluA$_3$) in PBS (pH=7.4) at 10 mg/mL.

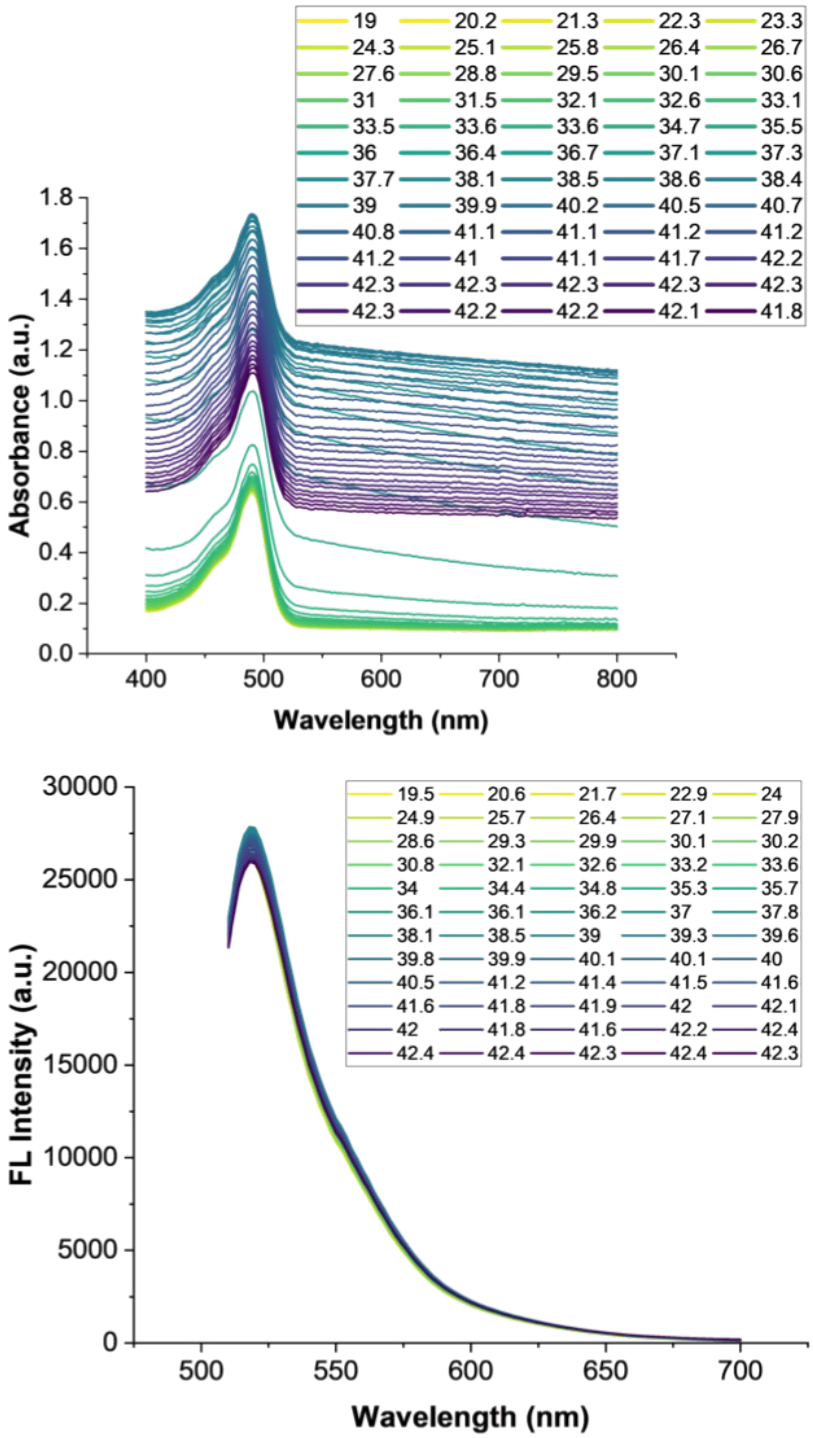

Figure S34. Temperature-dependent absorbance (top) and fluorescence emission spectrum (λ_{ex} = 490 nm) (bottom) of linear P(OEGMA$_{16}$-co-DEGMA$_{81}$-co-FluA$_3$) in PBS (pH=7.4) at 20 mg/mL.

4. Hyperbranched (HB) Thermoresponsive Fluorescent Polymers: Synthesis and Characterization

4.1. Synthesis of the Chain Transfer Monomer (CTM) Conjugates (CTDPA-HEMA)

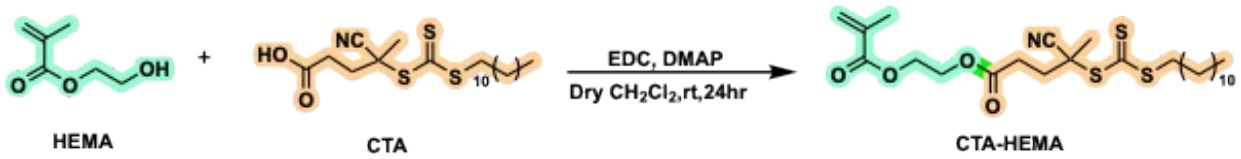

Scheme S4. Synthesis of chain transfer agent-2-hydroxyethyl methacrylate conjugate (CTDPA-HEMA) via Steglich Esterification

In a dry round-bottom flask equipped with a magnetic stir bar, chain transfer agent (CTDPA, 1.0 g, 2.48 mmol), 2-hydroxyethyl methacrylate (HEMA, 380 mg, 2.92 mmol), and 4-(dimethylamino)pyridine (DMAP, 32 mg, 0.26 mmol) were dissolved in 15 mL of anhydrous dichloromethane (CH_2Cl_2). The reaction mixture was cooled to 0 °C and stirred under a nitrogen atmosphere for 10 min. A solution of 1-ethyl-3-(3-dimethylaminopropyl)carbodiimide hydrochloride (EDC·HCl, 560 mg, 2.92 mmol) in 10 mL of dry CH_2Cl_2 was then added dropwise. The mixture was allowed to warm to room temperature and stirred for 24 h. After completion, the reaction mixture was filtered and washed with saturated aqueous NaCl solution. The organic layer was collected, dried over anhydrous $MgSO_4$, and filtered. The solvent was removed under reduced pressure, and the crude product was purified by silica gel flash column chromatography (hexanes/ethyl acetate = 5:1) to afford CTDPA-HEMA as a pale-yellow viscous oil (883 mg, 1.71 mmol, 69% yield).

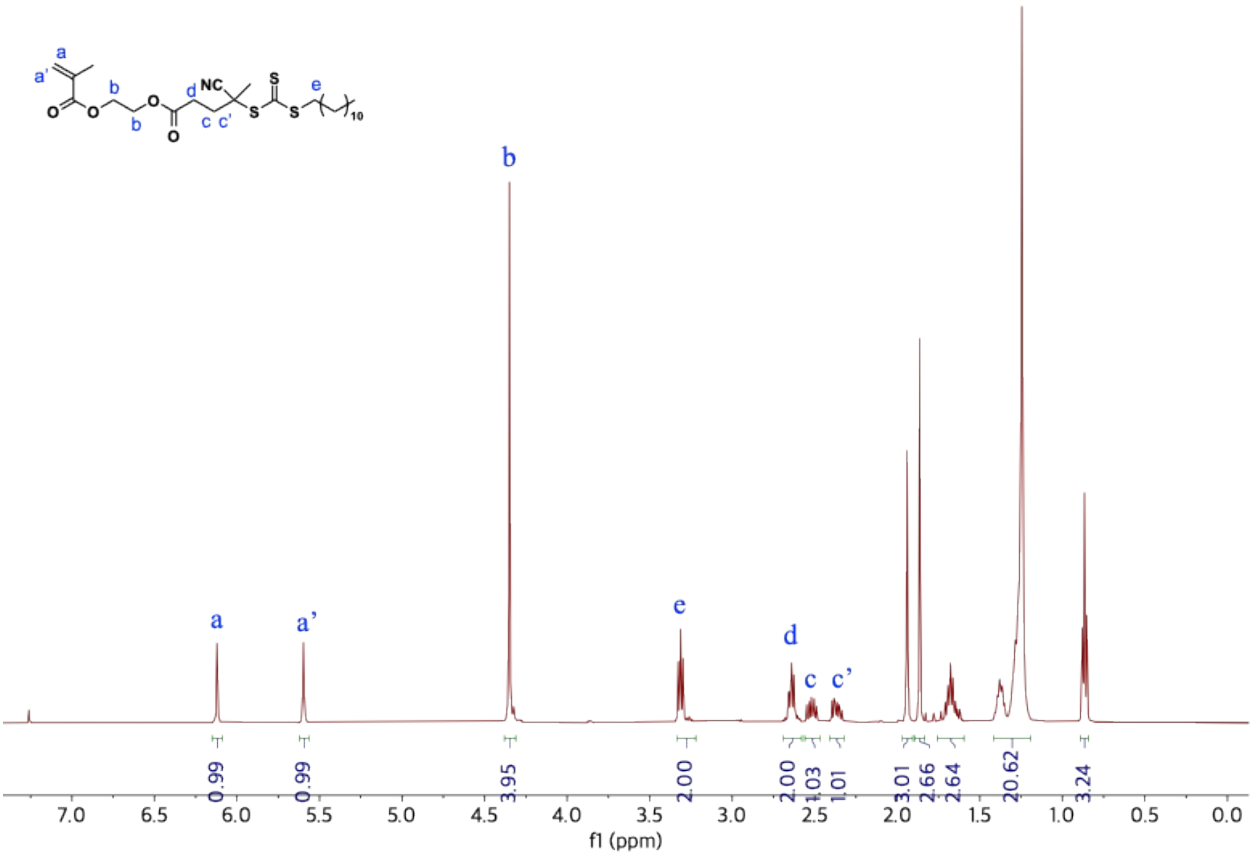

Figure S35. ^{1}H NMR spectrum of CTDPA-HEMA in $CDCl_3$.

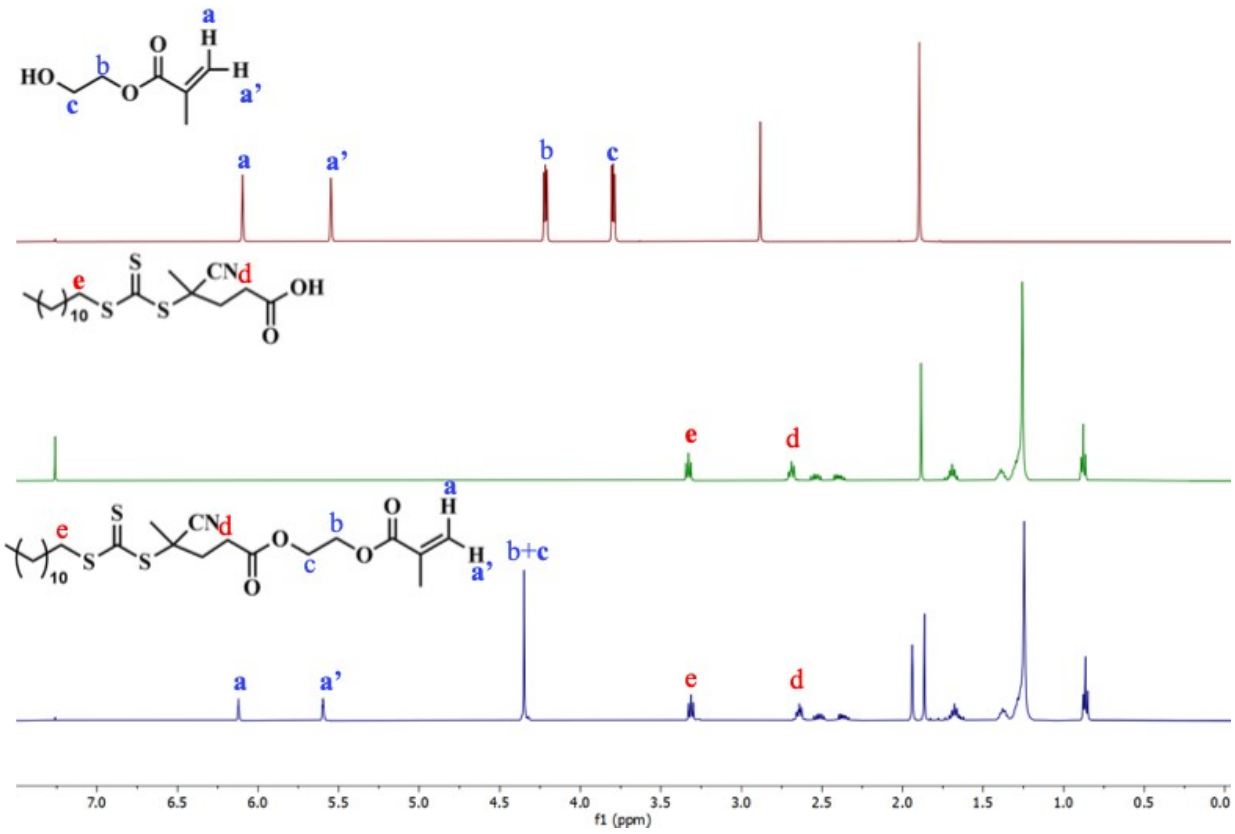

Figure S36. Overlayed ^{1}H NMR spectra of HEMA, CTDPA, and CTDPA-HEMA in $CDCl_3$.

4.2. HB P(NIPAM-*co*-CTDPA-HEMA-*co*-FluA) (Feed ratio = 94:5:1)

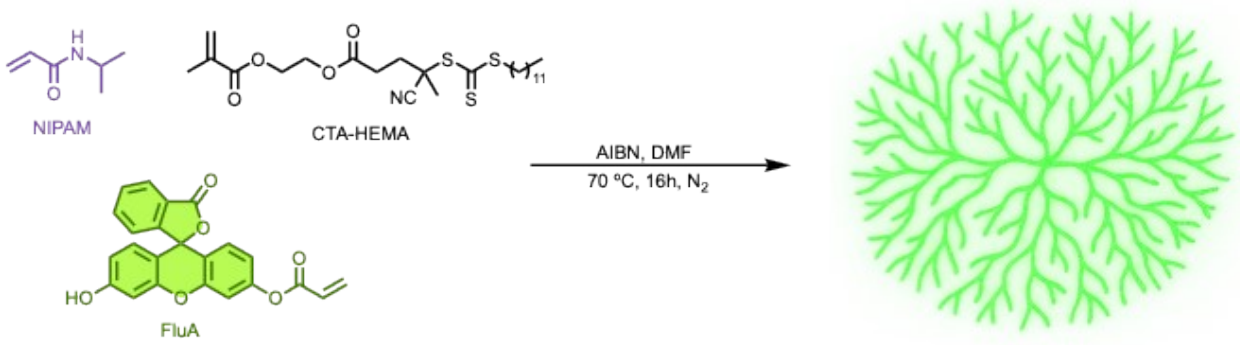

Scheme S5. Synthesis of HB P(NIPAM-*co*-CTDPA-HEMA-*co*-FluA) via RAFT polymerization.

Recrystallized NIPAM (201 mg, 1.78 mmol), FluA (7.2 mg, 0.02 mmol), CTDPA.HEMA (50 mg, 0.09 mmol), and AIBN (3.3 mg, 0.02 mmol) were dissolved in DMF (1 mL) in a 5mL Schlenk flask equipped with a Teflon-coated stir bar. The reaction mixture was deoxygenated by purging and sparging with N_2 for 10 min. After sparging, the Schlenk flask with the reaction mixture was heated at 70 °C for 19 hours. The obtained copolymer was purified by dissolving in methanol and

precipitating in hexanes three times and then dried under vacuum for further characterization, with an isolated yield of 0.24 g. Actual Composition = 90.6:5.7:3.7 by ^{1}H NMR Spectroscopy; SEC-MALS (DMF) characterization: M_n = 10.68 kDa, Đ = 1.3.

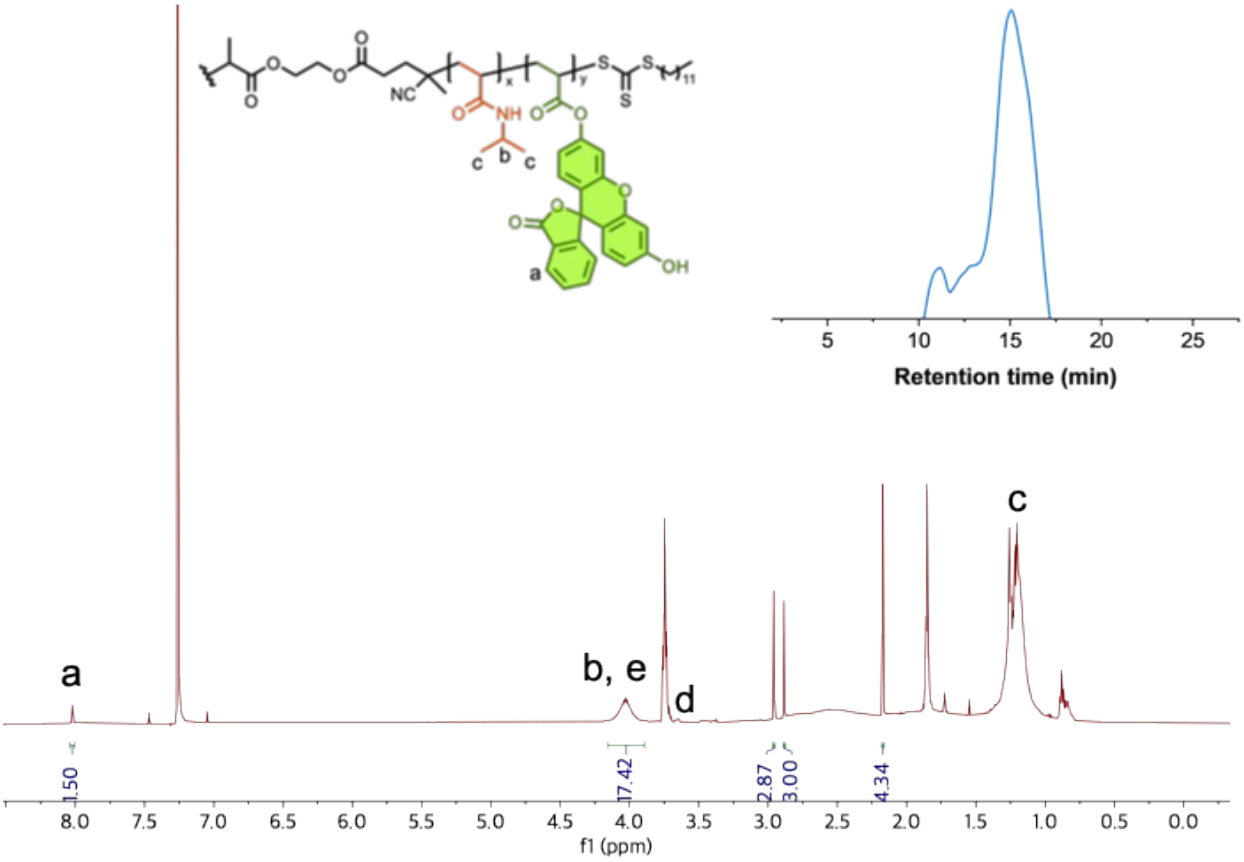

Figure S37. ^{1}H NMR spectrum in $CDCl_3$ and SEC-MALS (DMF) trace of HB P(NIPAM-*co*-CTDPA-HEMA-*co*-FluA).

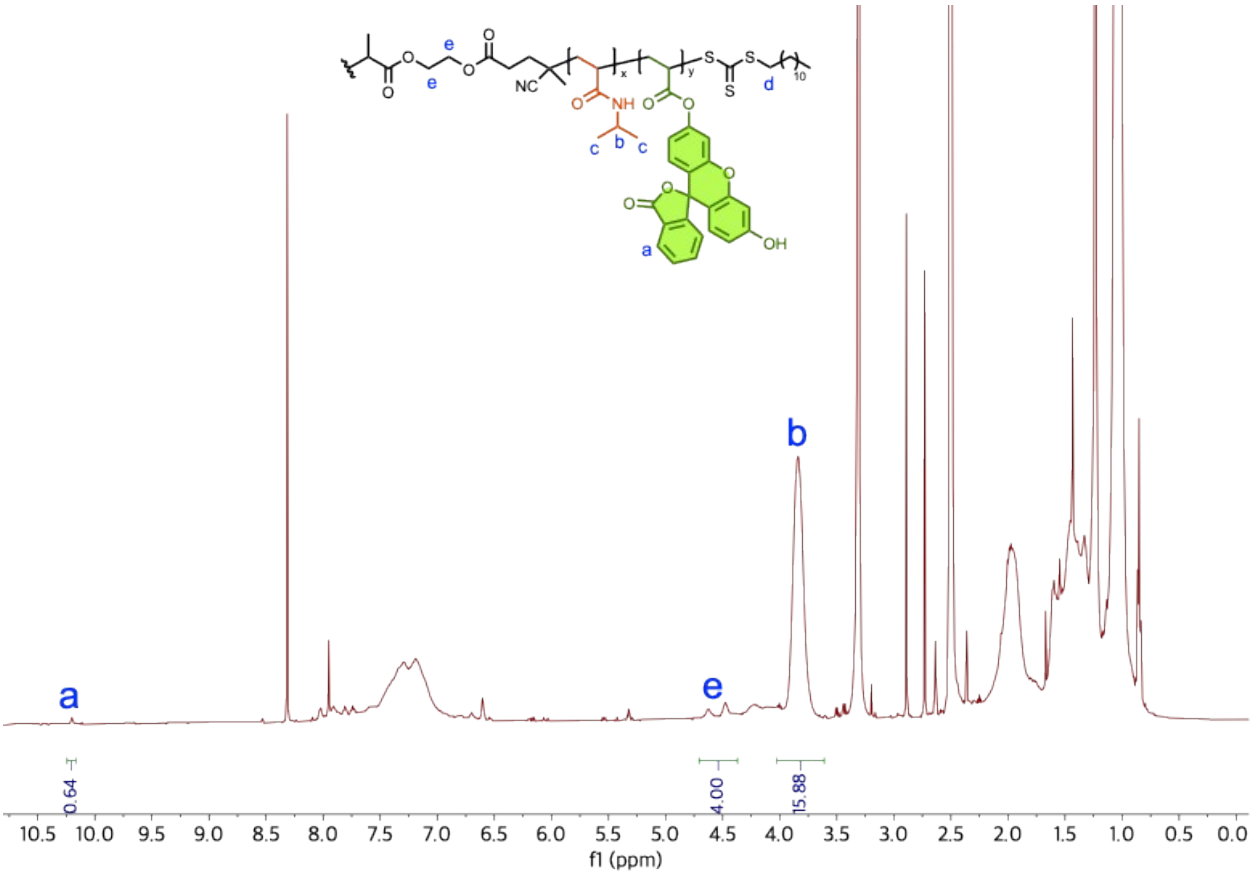

Figure S38. ^{1}H NMR spectrum of HB P(NIPAM-*co*-CTDPA-HEMA-*co*-FluA) in DMSO-d_6.

4.2.1. End Group Removal via AIBN

The purified HB polymer (95.4 mg, M_n = 10.7 kDa), AIBN (131.5 mg, 0.8 mmol), and THF (10.0 mL) were added to a 100 mL round-bottom flask equipped with a Teflon-coated magnetic stir bar. The reaction mixture was deoxygenated by N_2 sparging for 30 min, followed by reflux at 70 °C for 8 h under a N_2 atmosphere. After completion, the reaction mixture was cooled to room temperature, and the solvent was removed under reduced pressure using rotary evaporation. The resulting residue was washed with hexane three times to afford the final product.

4.2.2. End Group Removal via ACVA

The purified HB polymer (73.1 mg, M_n = 10.7 kDa), ACVA (168.2 mg, 0.6 mmol), and THF (10.0 mL) were added to a 100 mL round-bottom flask equipped with a Teflon-coated magnetic stir bar. The reaction mixture was deoxygenated by N_2 sparging for 30 min, followed by reflux at 70 °C for 8 h under a N_2 atmosphere. After completion, the reaction mixture was cooled to room temperature, and the solvent was removed under reduced pressure using rotary evaporation. The resulting residue was washed with hexanes three times to afford the final product.

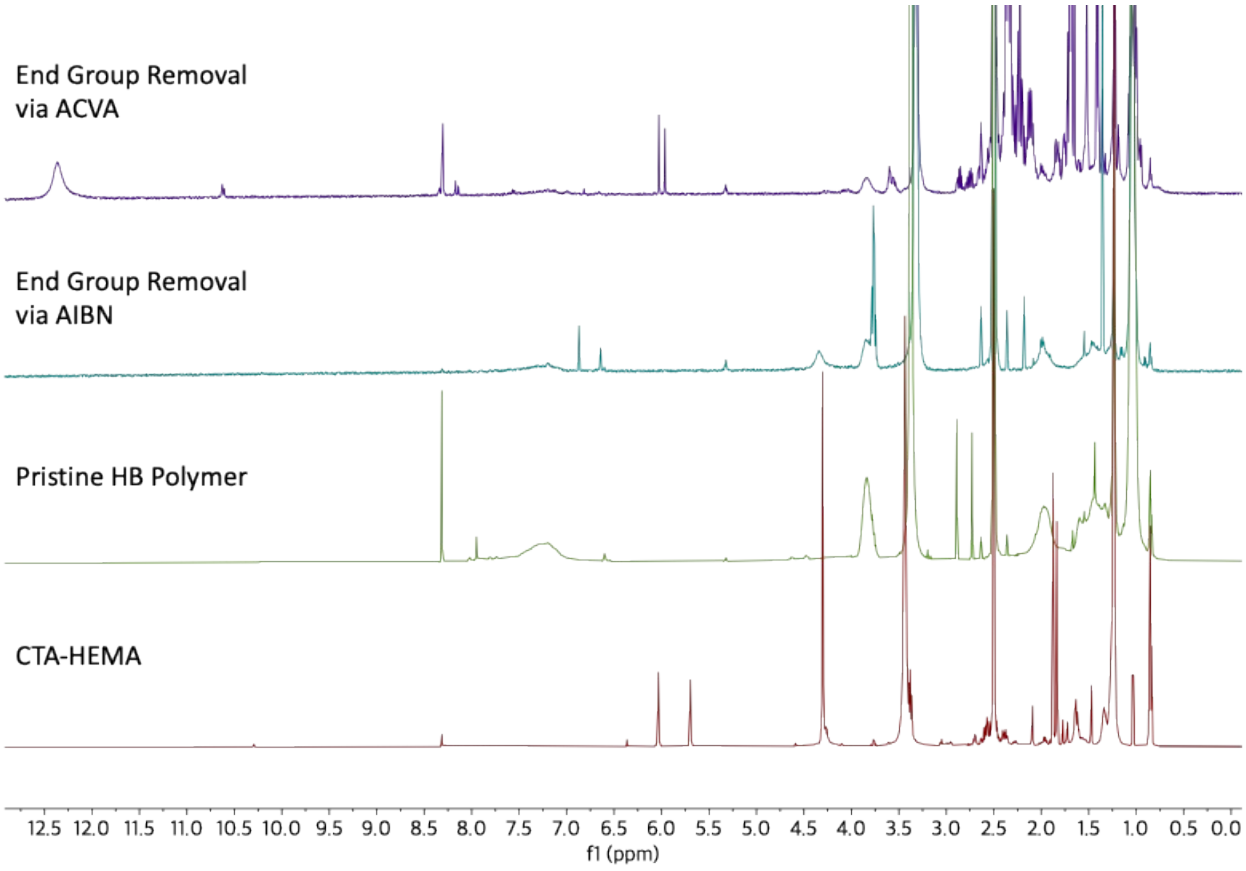

Figure S39. Overlaid spectra of CTDPA-HEMA, pristine polymer HB P(NIPAM-*co*-CTDPA-HEMA-*co*-FluA), and end group removed polymers in DMSO-d_6.

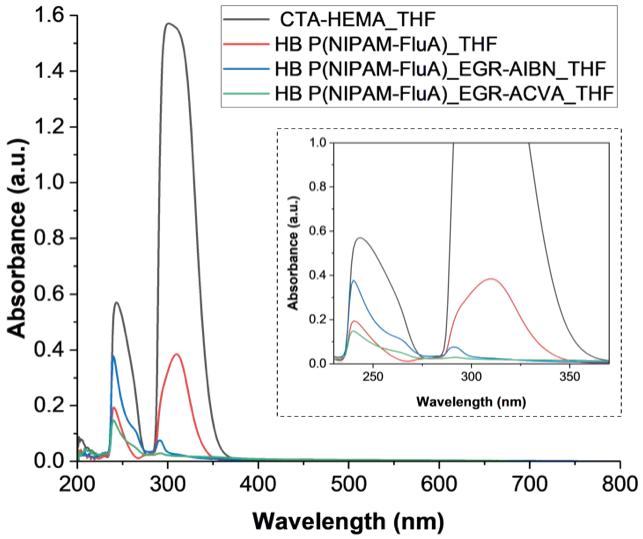

Figure S40. UV-Vis spectra of HB P(NIPAM-*co*-CTDPA-HEMA-*co*-FluA) before and after end group removal via AIBN and ACVA, in THF at 0.1 mg/mL.

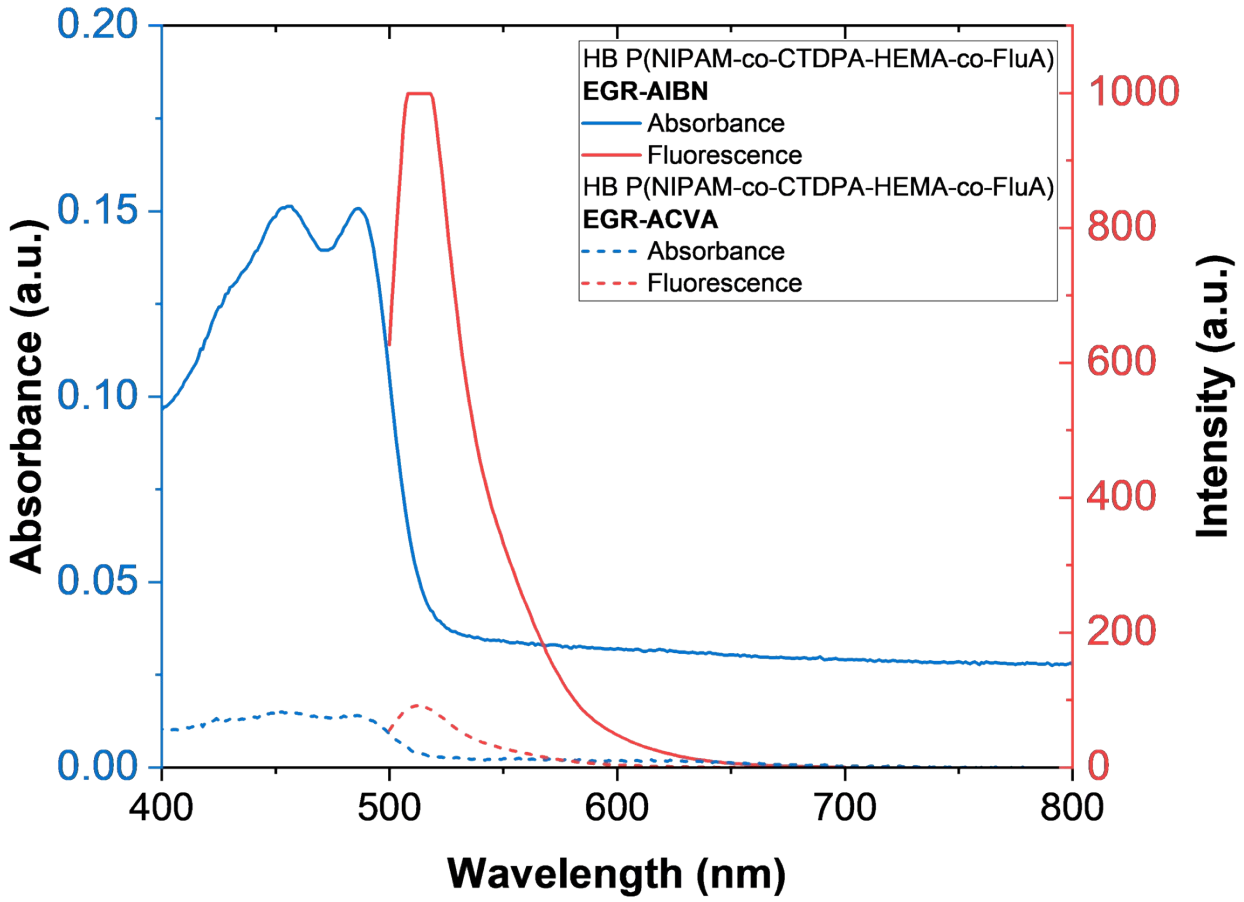

Figure S41. Absorbance and fluorescence spectra of HB P(NIPAM-*co*-CTDPA.HEMA-*co*-FluA) after end group removal via AIBN and ACVA, in PBS at 0.1 mg/mL.

4.3. HB P(TEGMA-*co*-CTDPA.HEMA-*co*- FluA) (Feed ratio = 94:5:1)

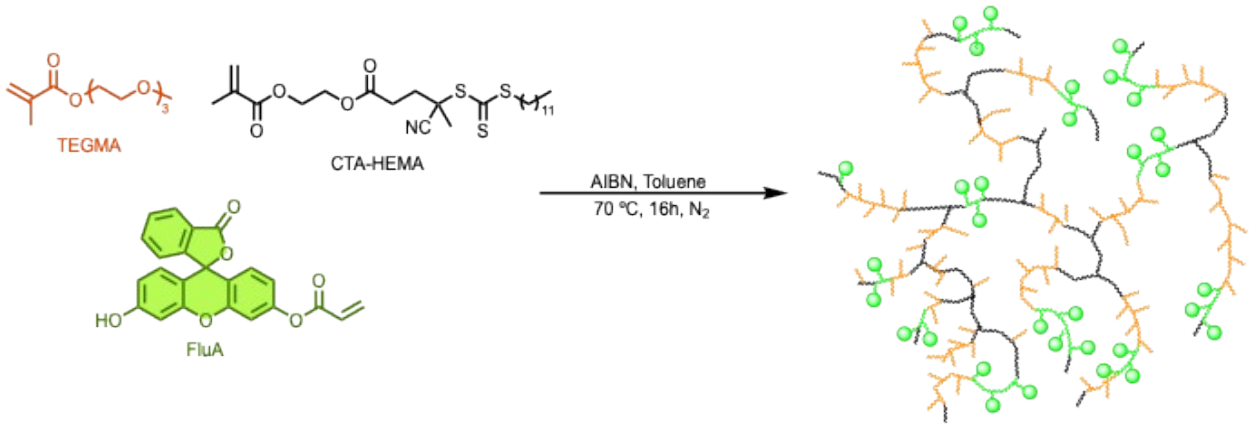

Scheme S6. Synthesis of HB P(NIPAM-*co*-CTDPA-HEMA-*co*-FluA) via RAFT polymerization.

Purified TEGMA (0.5 mL, 2.21 mmol), FluA (9.4 mg, 0.02 mmol), CTDPA.HEMA (61.9 mg, 0.12 mmol), and AIBN (4 mg, 0.02 mmol) were dissolved in toluene (0.5 mL) in a 5 mL Schlenk flask equipped with a Teflon-coated stir bar. The reaction mixture was deoxygenated by purging and sparging with N_2 for 10 min. After sparging, the Schlenk flask with the reaction mixture was heated at 70 °C for 19 hours. The obtained terpolymer was purified by precipitating in hexanes three times and then dried under vacuum for further characterization, with an isolated yield of 0.65 g. Actual Composition = 92.9:3.6:3.5 by ^{1}H NMR Spectroscopy. SEC-MALS (DMF) characterization: M_n = 40 kDa, Đ = 2.1.

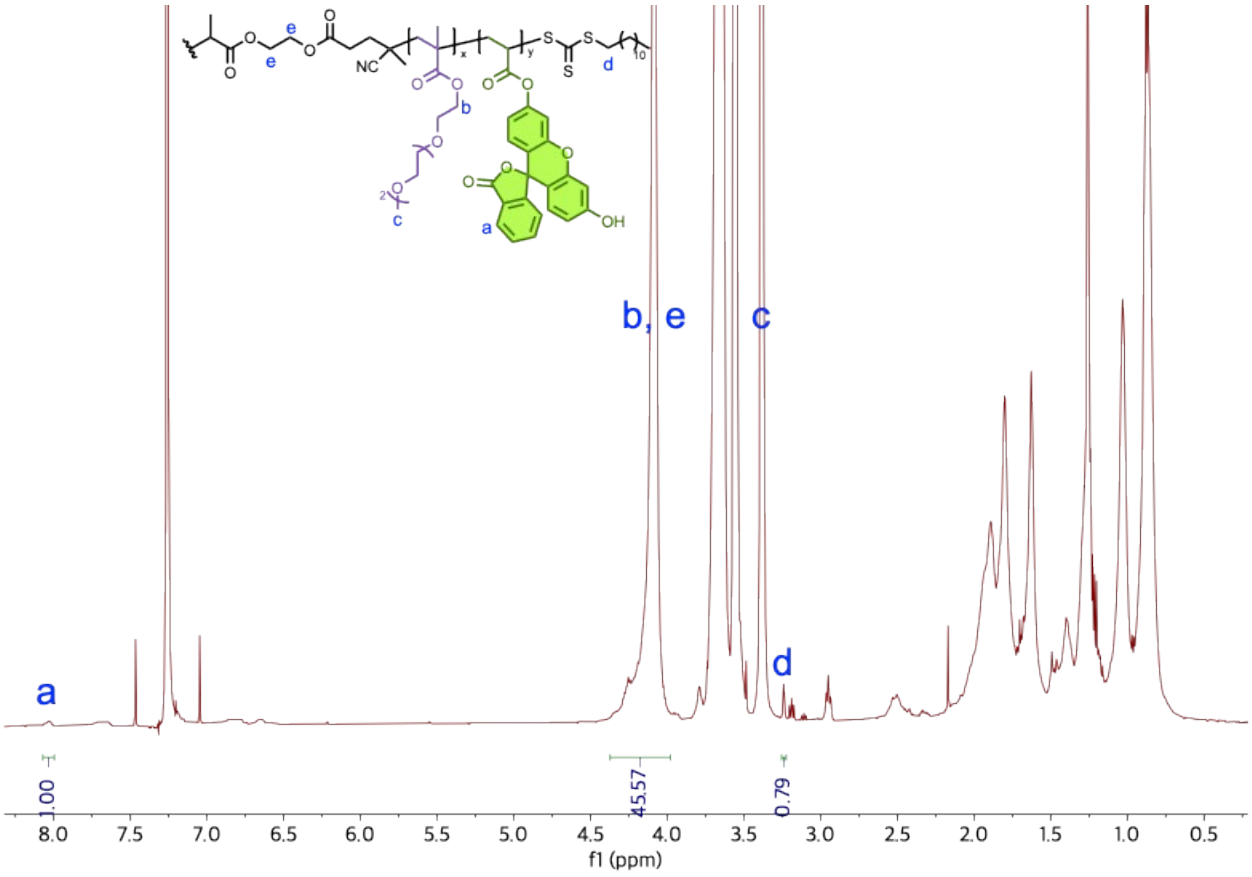

Figure S42. ^{1}H NMR spectrum of HB P(TEGMA$_{92.9}$-*co*-CTDPA-HEMA$_{3.6}$-*co*-FluA$_{3.5}$) in $CDCl_3$.

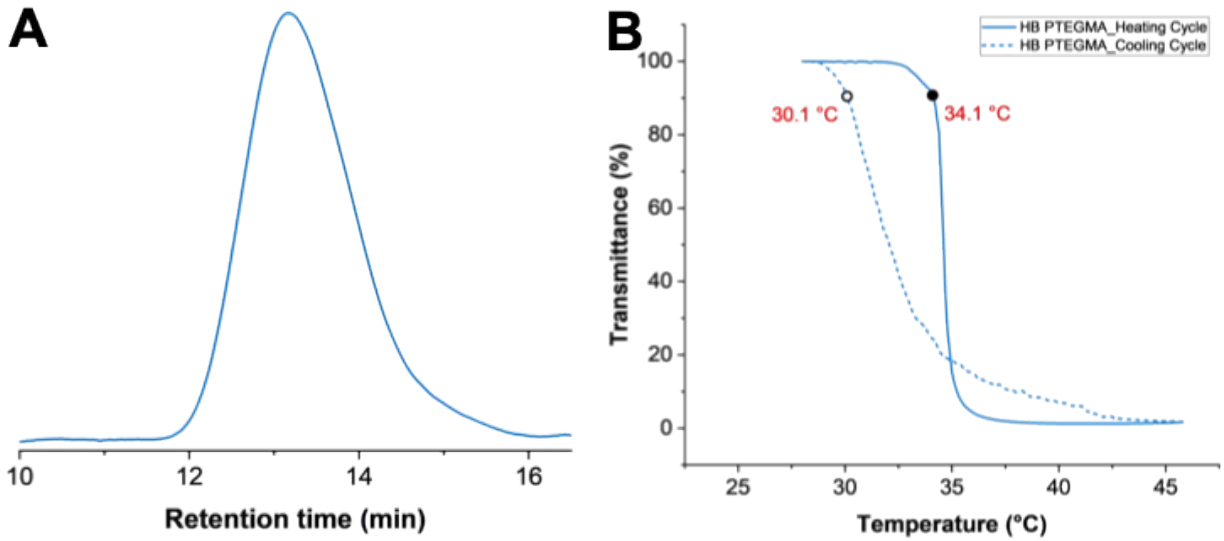

Figure S43. **(A)** SEC-MALS (DMF) trace, **(B)** absorbance and fluorescence at 0.1 mg/mL, and **(C)** cloud point temperature profile at 10 mg/mL of HB P(TEGMA$_{92.9}$-*co*-CTDPA-HEMA$_{3.6}$-*co*-FluA$_{3.5}$) synthesized via RAFT polymerization.

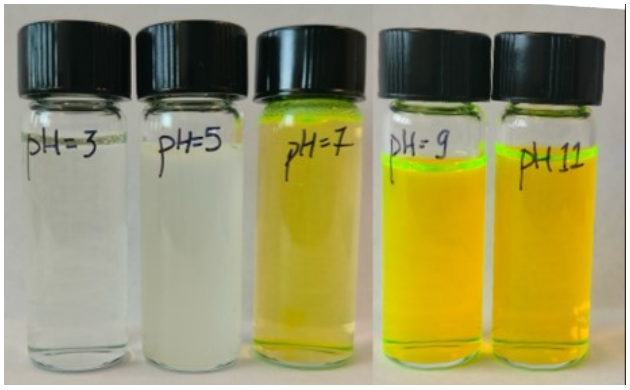

Figure S44. Visual comparison of HB P(TEGMA$_{92.9}$-*co*-CTDPA-HEMA$_{3.6}$-*co*-FluA$_{3.5}$) solubility/behavior in solutions of varying pH (3, 5, 7.4, 9, 11)

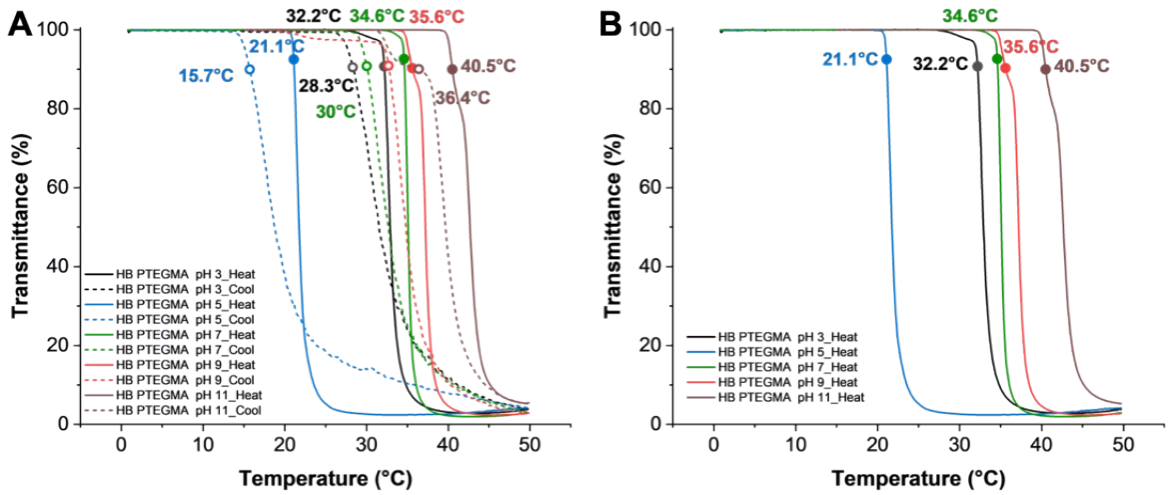

Figure S45. **(A)** Cloud point temperature profiles of linear HB P(TEGMA$_{92.9}$-*co*-CTDPA-HEMA$_{3.6}$-*co*-FluA$_{3.5}$) at varying pH at 5 mg/mL with heating and cooling cycles, **(B)** without cooling cycles.

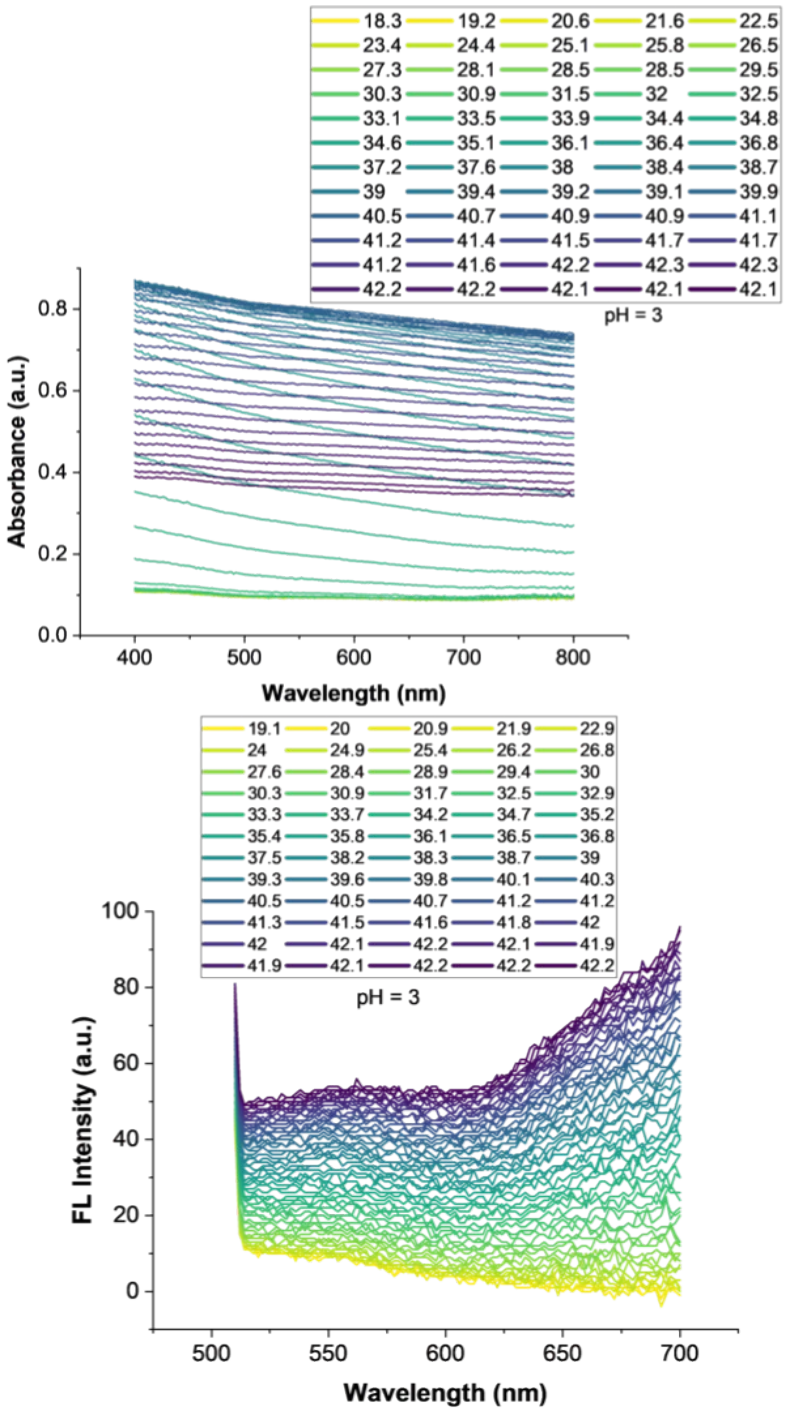

Figure S46. Temperature-dependent absorbance (top) and fluorescence emission spectrum (λ_{ex} = 490 nm) (bottom) of HB P(TEGMA$_{92.9}$-*co*-CTDPA-HEMA$_{3.6}$-*co*-FluA$_{3.5}$) at pH=3 at 5 mg/mL.

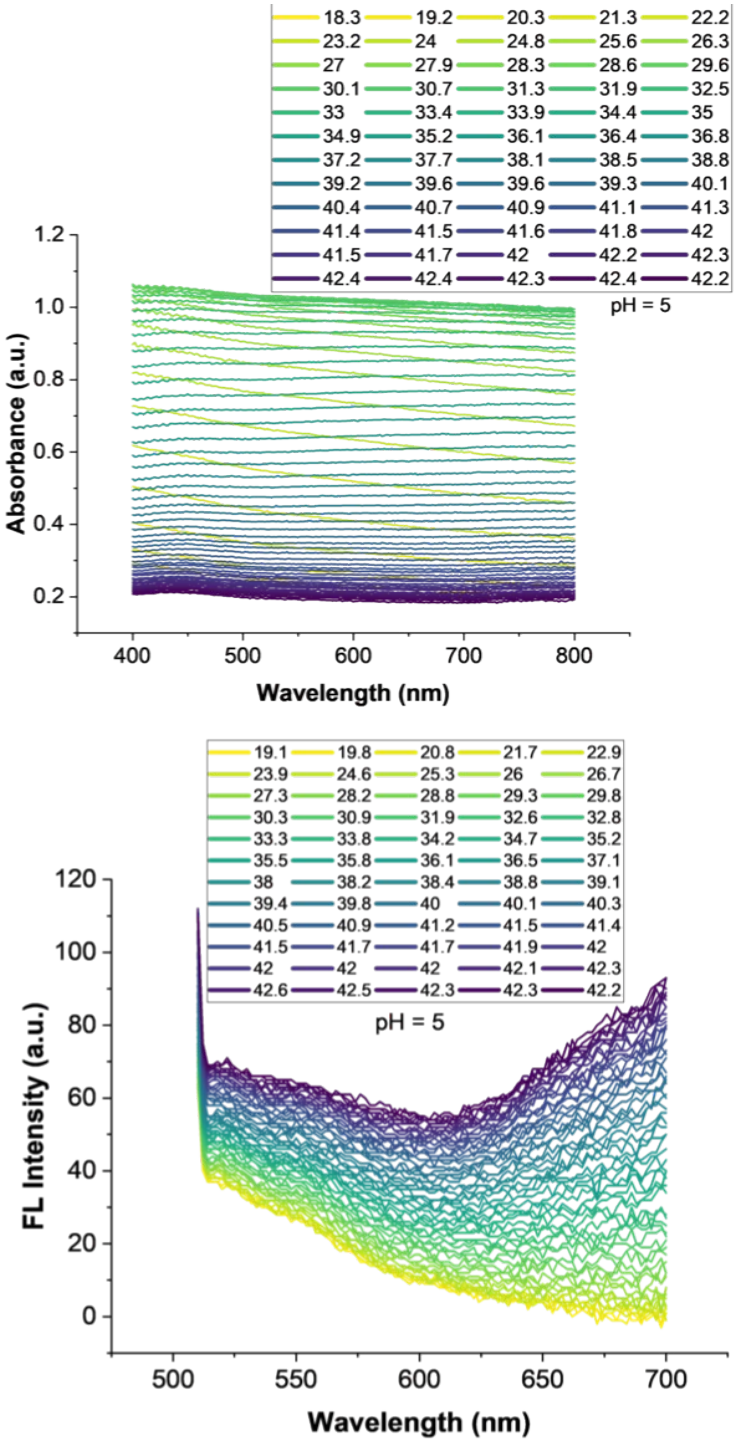

Figure S47. Temperature-dependent absorbance (top) and fluorescence emission spectrum (λ_{ex} = 490 nm) (bottom) of HB P(TEGMA$_{92.9}$-*co*-CTDPA-HEMA$_{3.6}$-*co*-FluA$_{3.5}$) at pH=5 at 5 mg/mL.

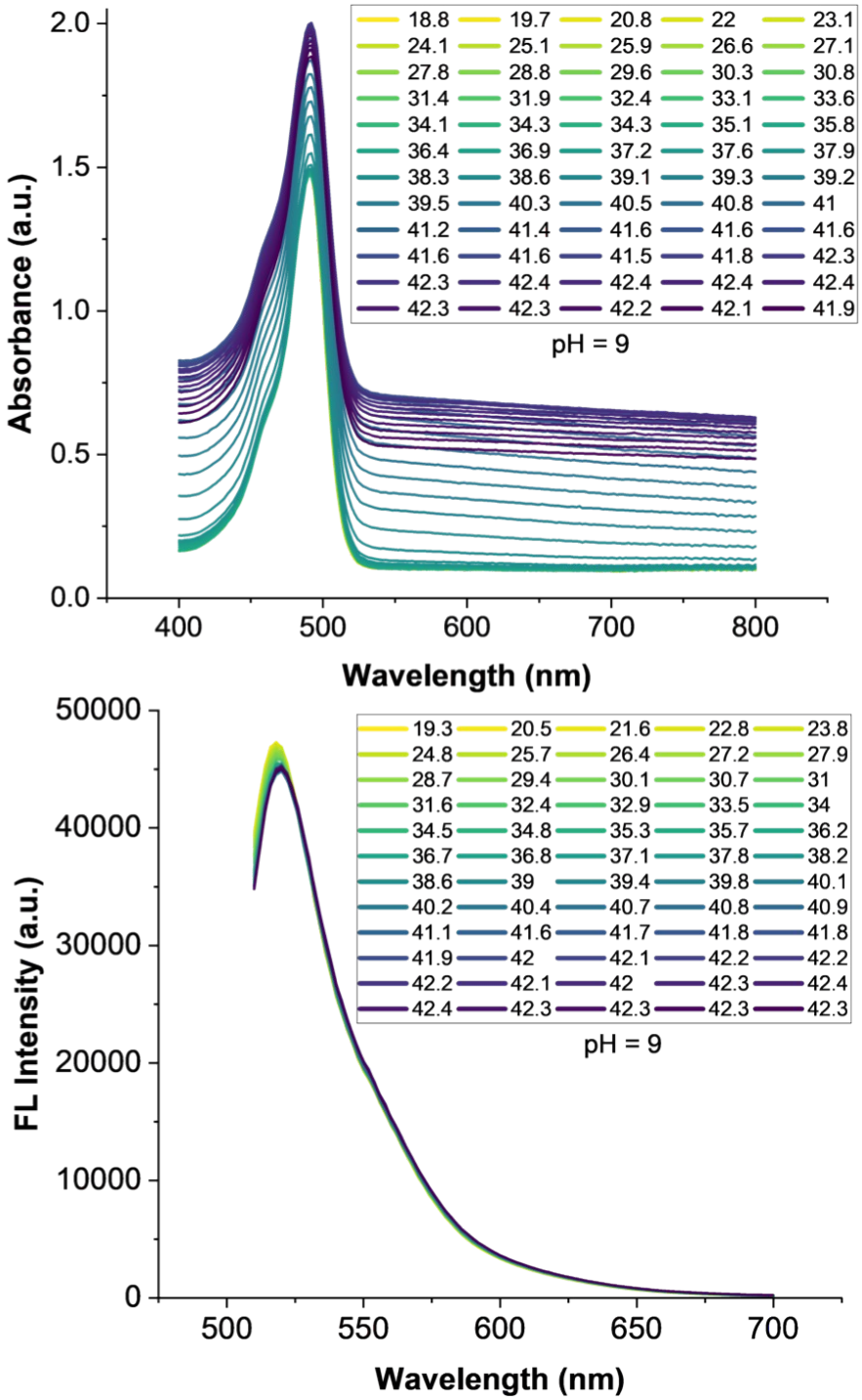

Figure S48. Temperature-dependent absorbance (top) and fluorescence emission spectrum (λ_{ex} = 490 nm) (bottom) of HB P(TEGMA$_{92.9}$-*co*-CTDPA-HEMA$_{3.6}$-*co*-FluA$_{3.5}$) at pH=9 at 5 mg/mL.

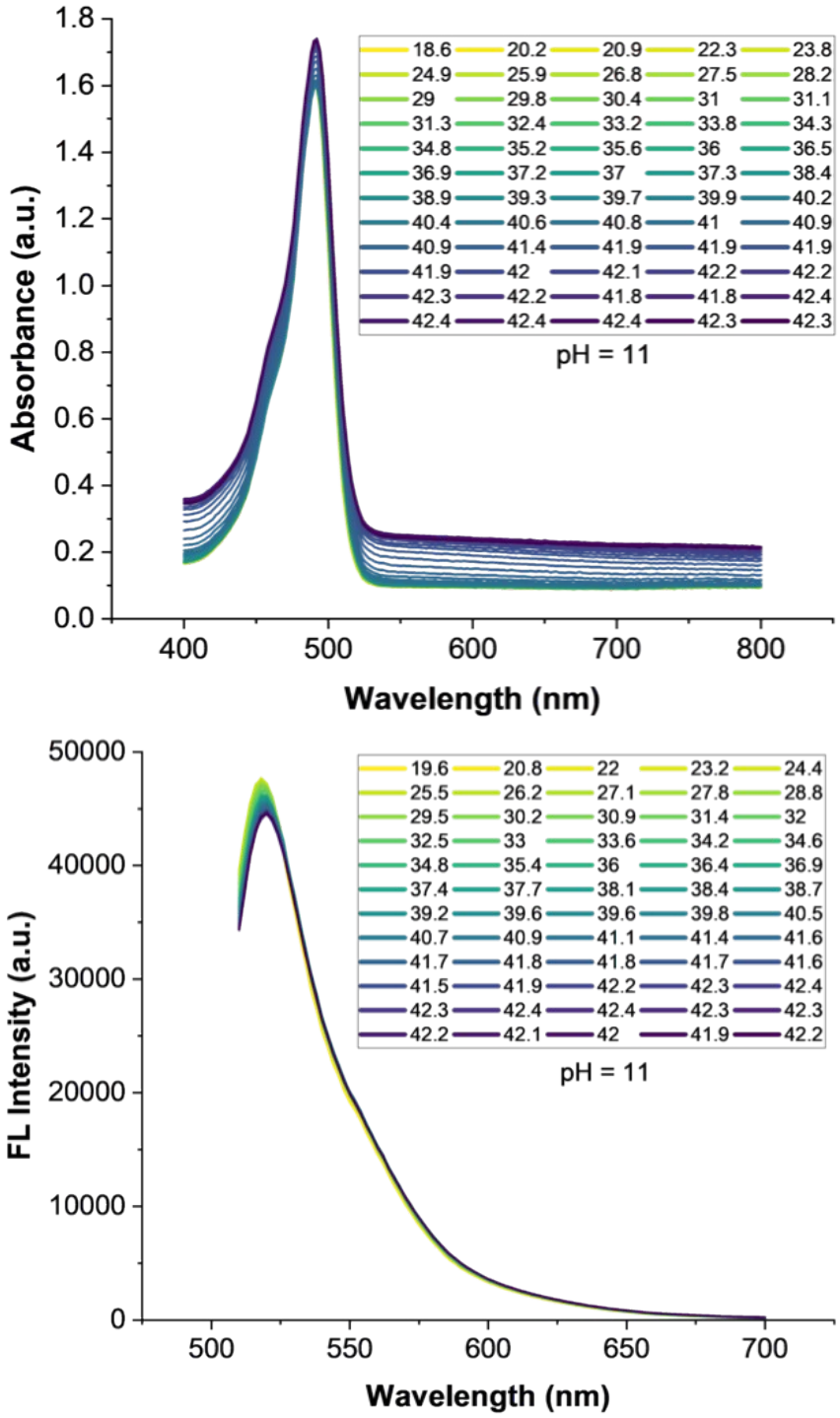

Figure S49. Temperature-dependent absorbance (top) and fluorescence emission spectrum (λ_{ex} = 490 nm) (bottom) of HB P(TEGMA$_{92.9}$-*co*-CTDPA-HEMA$_{3.6}$-*co*-FluA$_{3.5}$) at pH=11 at 5 mg/mL.

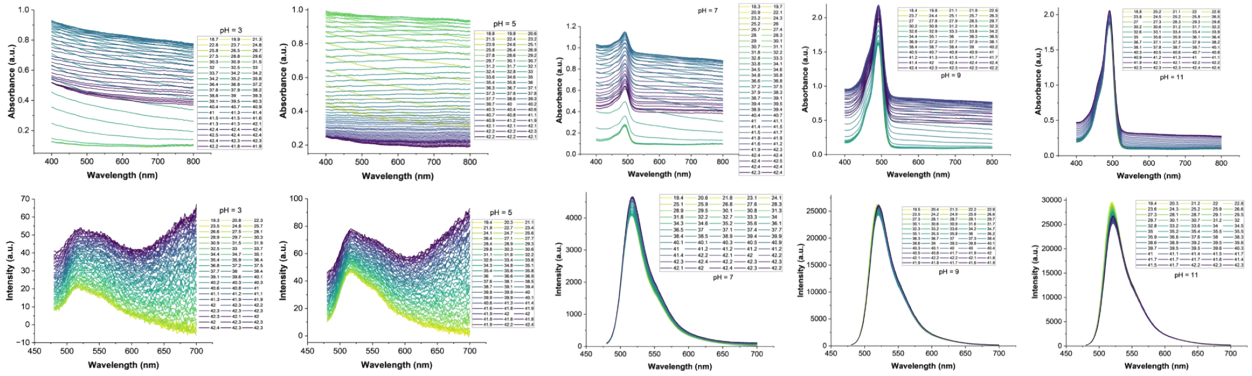

Figure S50. Temperature-dependent absorbance and fluorescence of HB P(TEGMA$_{92.9}$-*co*-CTDPA-HEMA$_{3.6}$-*co*-FluA$_{3.5}$) at varying pH (pH = 3, 5, 7.4, 9 and 11) at 5 mg/mL when excited at 450 nm (λ_{ex}) to get the full fluorescence spectrum.

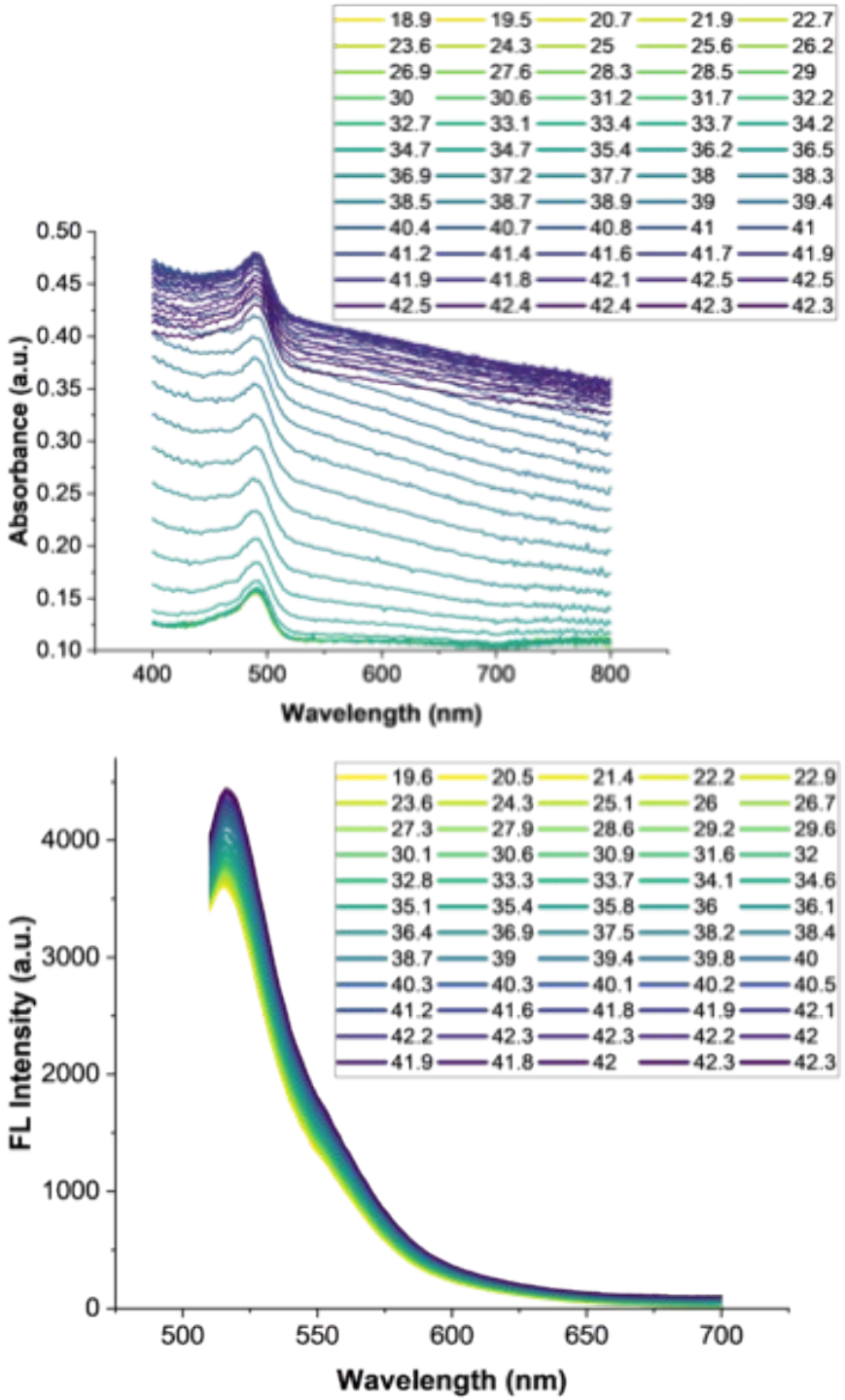

Figure S51. Temperature-dependent absorbance (top) and fluorescence emission spectrum (λ_{ex} = 490 nm) (bottom) of HB P(TEGMA$_{92.9}$-*co*-CTDPA-HEMA$_{3.6}$-*co*-FluA$_{3.5}$) in PBS (pH=7.4) at 1 mg/mL.

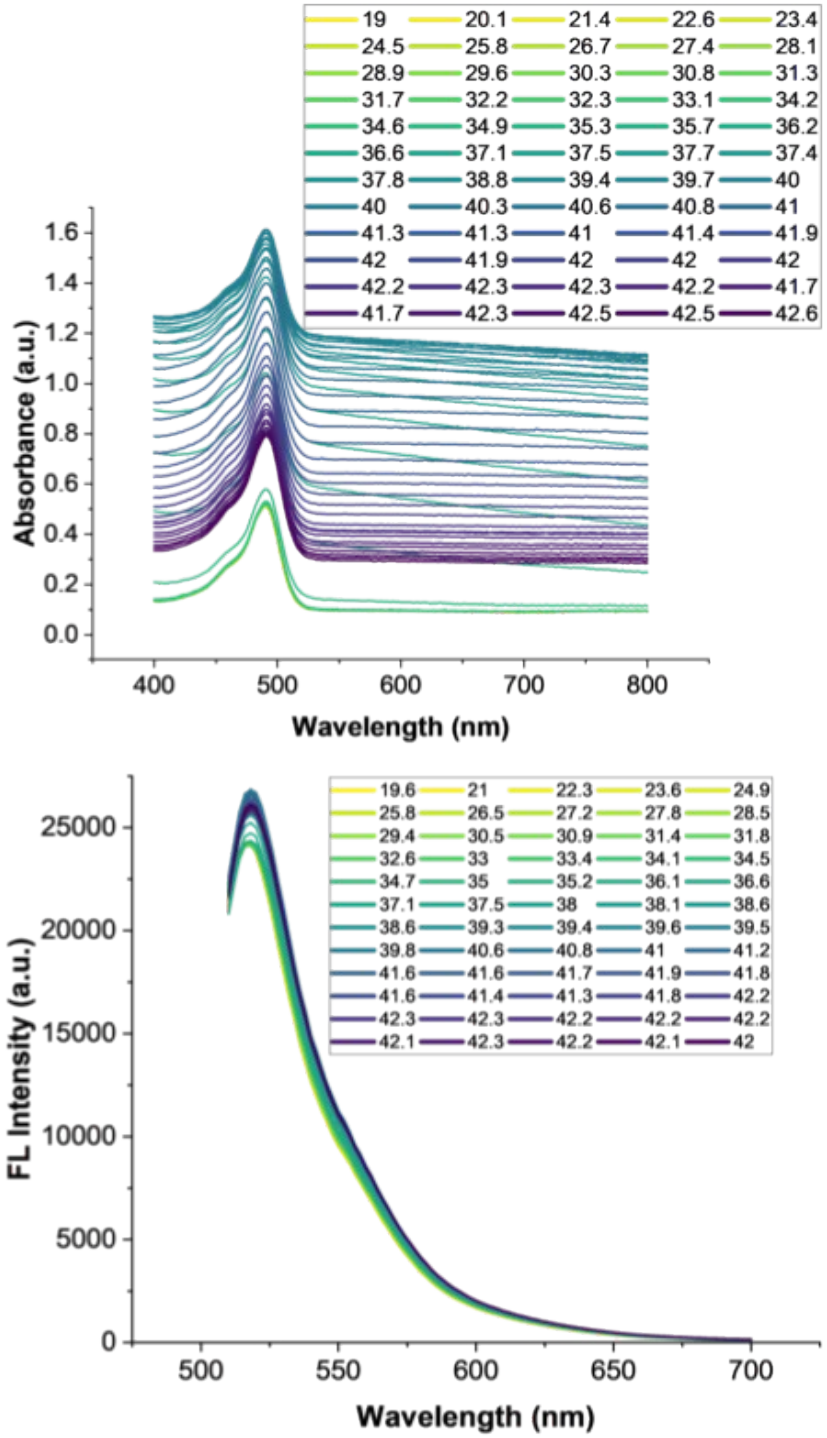

Figure S52. Temperature-dependent absorbance (top) and fluorescence emission spectrum (λ_{ex} = 490 nm) (bottom) of HB P(TEGMA$_{92.9}$-*co*-CTDPA-HEMA$_{3.6}$-*co*-FluA$_{3.5}$) in PBS (pH=7.4) at 10 mg/mL.

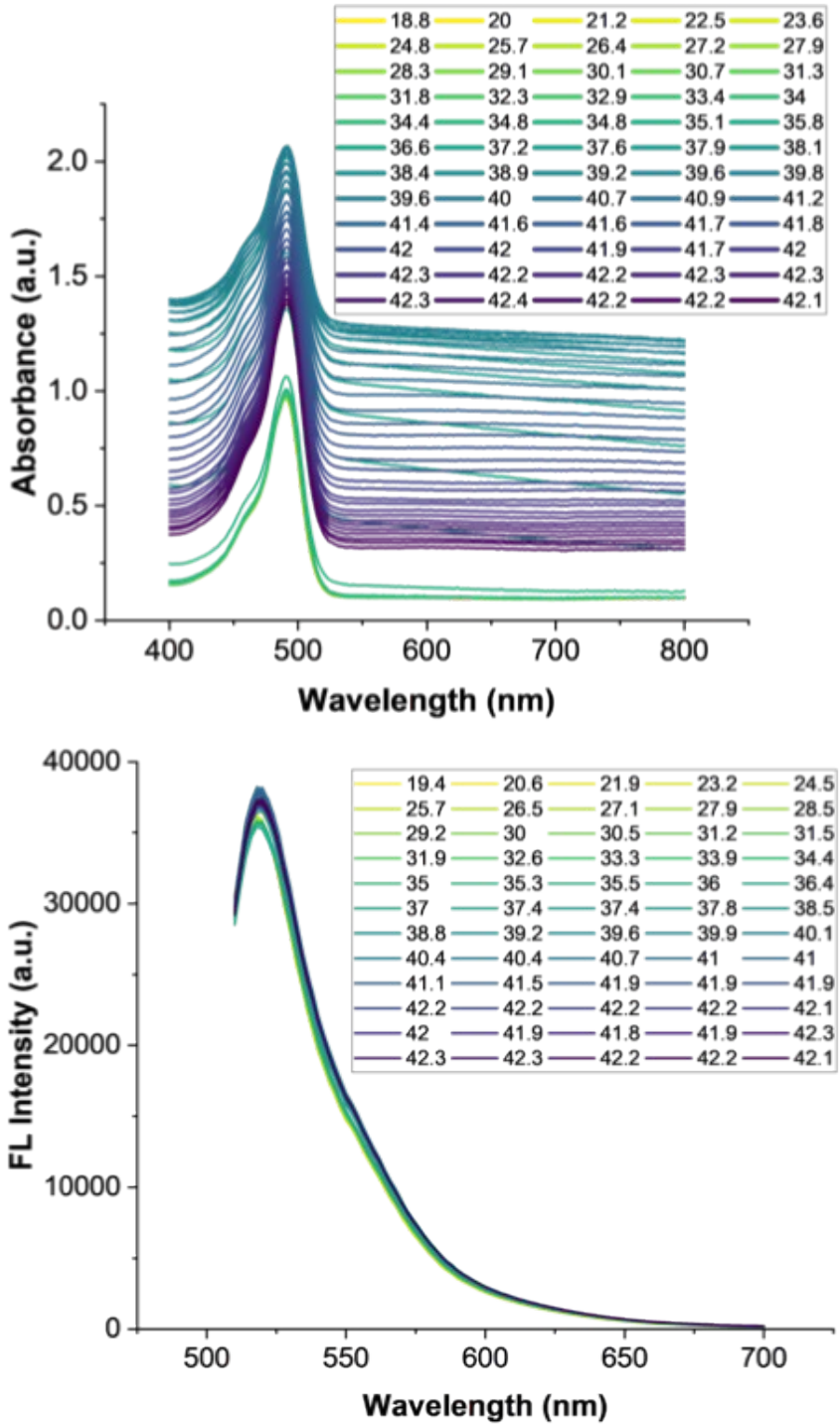

Figure S53. Temperature-dependent absorbance (top) and fluorescence emission spectrum (λ_{ex} = 490 nm) (bottom) of HB P(TEGMA$_{92.9}$-*co*-CTDPA-HEMA$_{3.6}$-co-FluA$_{3.5}$) in PBS (pH=7.4) at 20 mg/mL.

4.3.1. Linear PTEGMA via RAFT Polymerization as a Benchmark to Compare with HB P(TEGMA-*co*-CTDPA-HEMA-*co*-FluA)

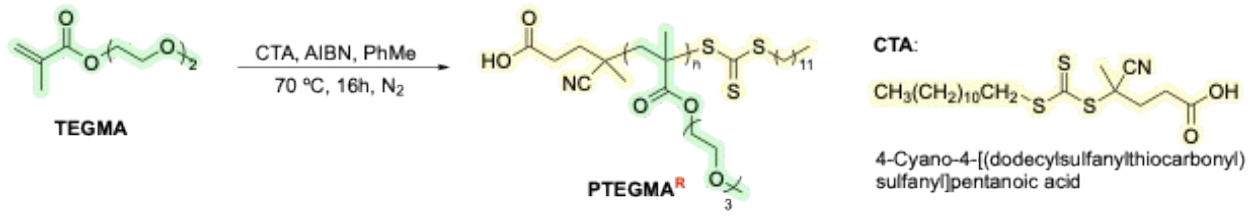

Scheme S7. Synthesis of linear PTEGMA via RAFT polymerization.

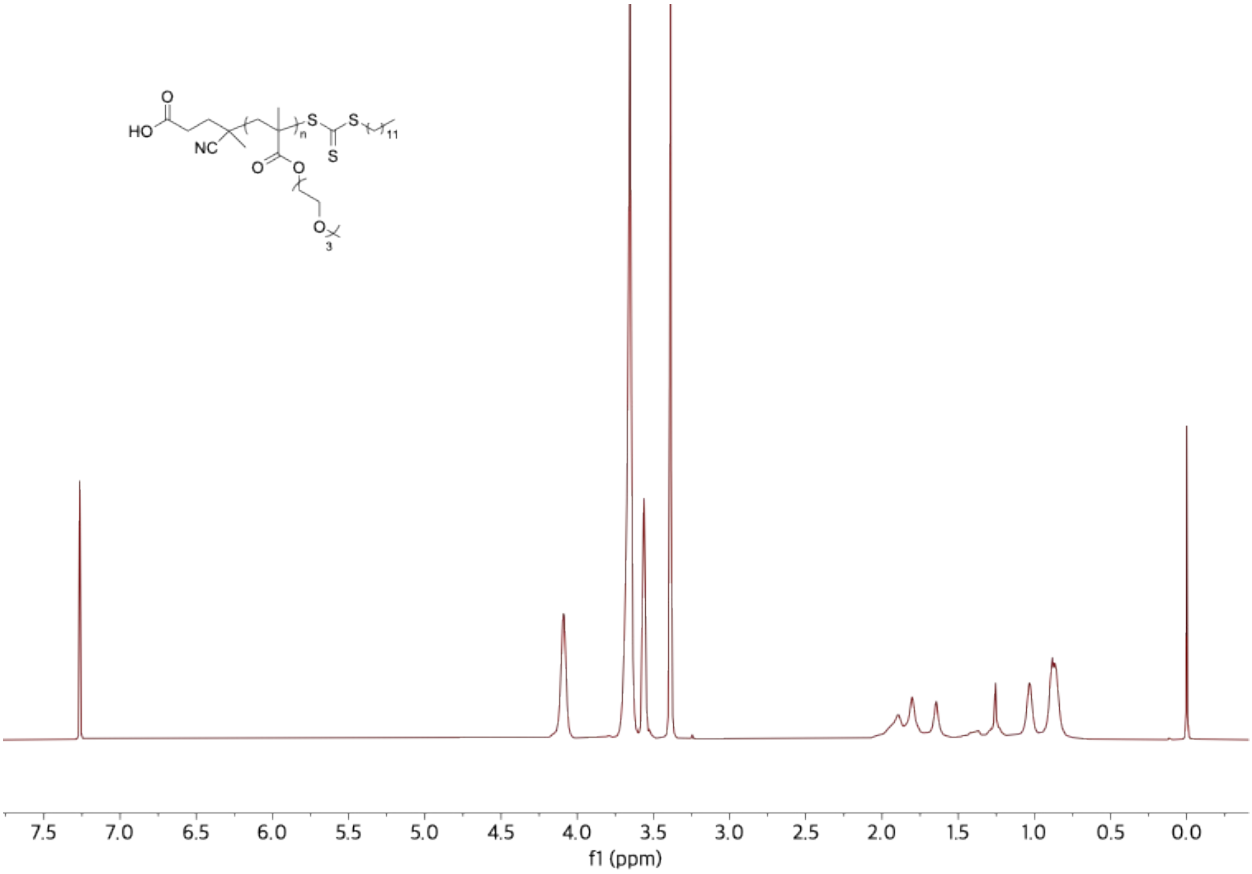

Figure S54. ^{1}H NMR spectrum of linear P(TEGMA) in CDCl3.

Purified TEGMA (151.0 mg, 0.65 mmol), CTA (3 mg, 0.0065 mmol), and AIBN (1.2 mg, 0.0065 mmol) were dissolved in toluene (0.3 mL) in a 10 mL Schlenk flask equipped with a Teflon-coated stir bar. The reaction mixture was deoxygenated by purging and sparging with N_2 for 10 min. After sparging, the Schlenk flask with the reaction mixture was heated at 70 °C for 19 hours. The obtained terpolymer was purified by precipitating in hexanes three times and then dried under vacuum for further characterization, with an isolated yield of 132 mg. SEC-MALS (DMF) characterization: M_n = 10.02 kDa, Đ = 1.29. T_{cp} = 48 °C.

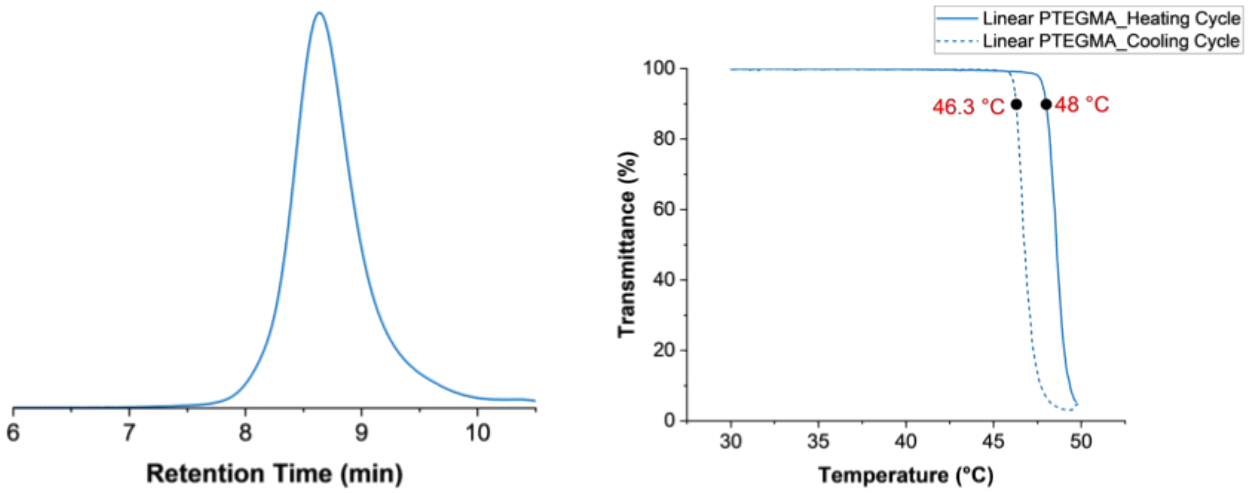

Figure S55. SEC (THF) trace (left) and cloud point temperature profile at 10 mg/mL (right) of linear PTEGMA synthesized via RAFT polymerization.

5. Temperature-dependent Fluorescence Measurements

5.1. Fluorescein Only

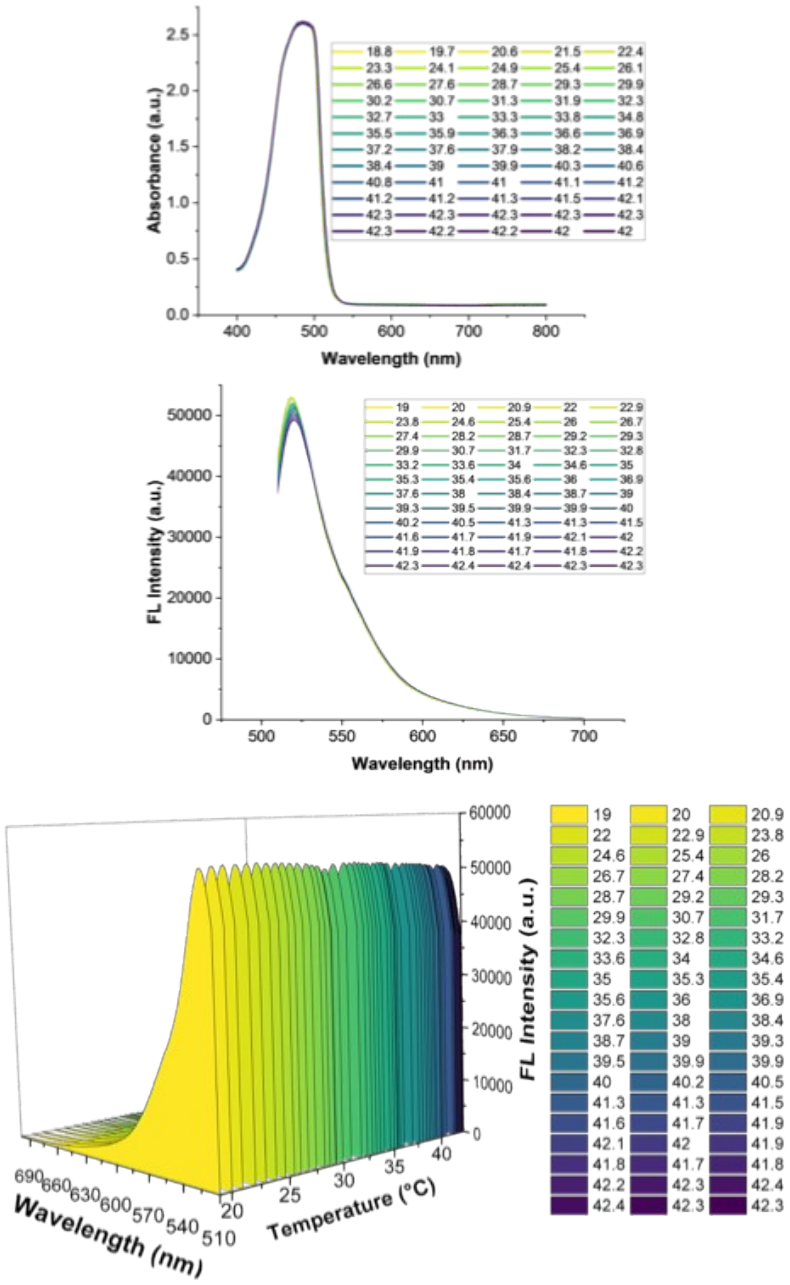

Figure S56. Temperature-dependent absorbance (top) and fluorescence emission spectrum (λ_{ex} = 490 nm) (middle), and 3D representation for fluorescence emission spectrum (λ_{ex} = 490 nm) (bottom) of Fluorescein in PBS (pH=7.4) at 0.25 mg/mL.

5.2. Mixture of Fluorescein and Linear PNIPAM (synthesized via RAFT)

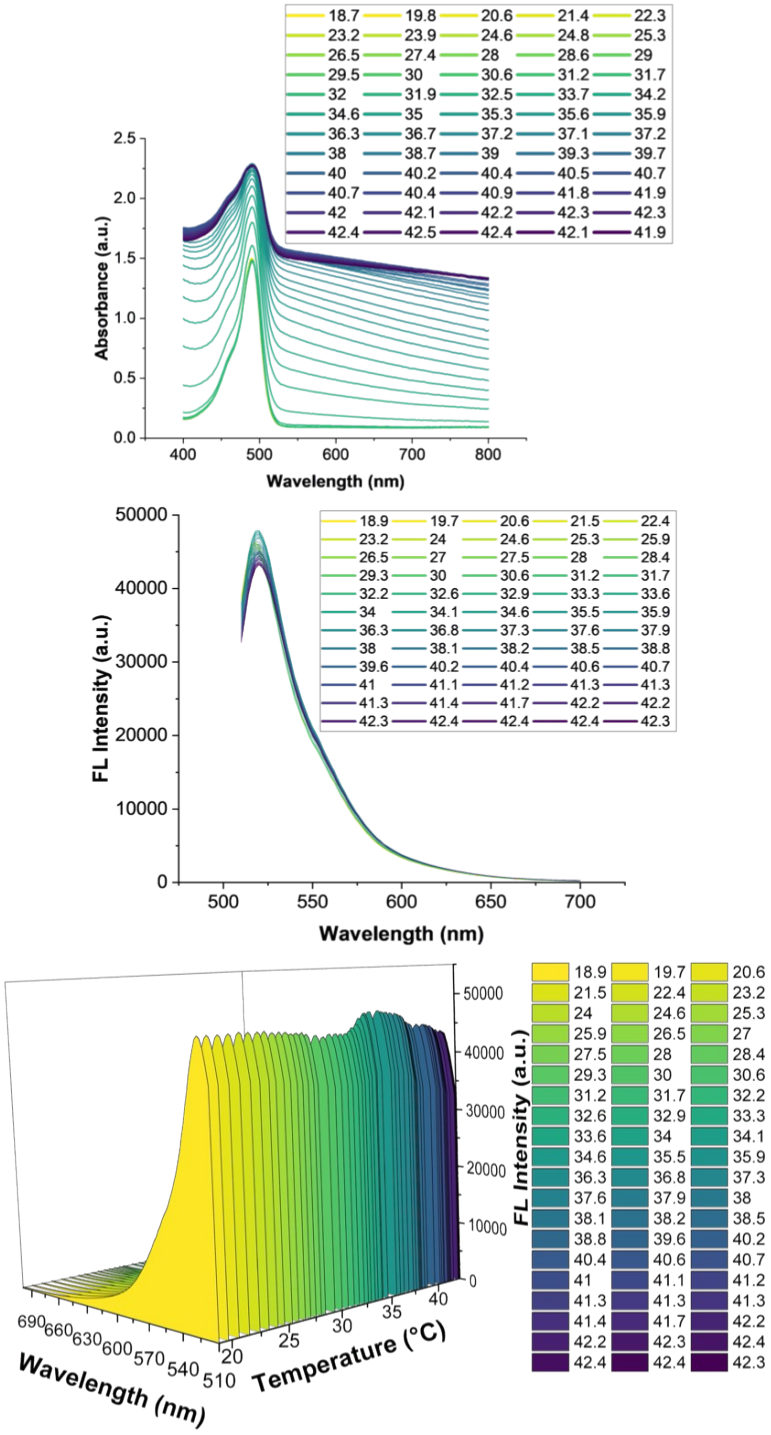

Figure S57. Temperature-dependent absorbance (top) and fluorescence emission spectrum (λ_{ex} = 490 nm) (middle), and 3D representation for fluorescence emission spectrum (λ_{ex} = 490 nm) (bottom) for a mixture of Fluorescein (0.25%) and linear PNIPAM synthesized via RAFT (4.75%) in PBS (pH=7.4) at 5 mg/mL.

6. Miscellaneous Figures

Acronym	FluA per chain	[FluA] (mM, 5 mg/mL)	[FluA] (μM, 0.1 mg/mL)
$LP_{NIPAM}5$	~139	2.0	40.4
$LP_{NIPAM}1$	~87	1.6	35.6
$HBP_{NIPAM}1$	-	-	-
$LP_{EGMA}5$	~54	2.39	47.8
$LP_{EGMA}1$	~23	0.59	11.8
$HBP_{EGMA}1$	~6	0.71	14.2

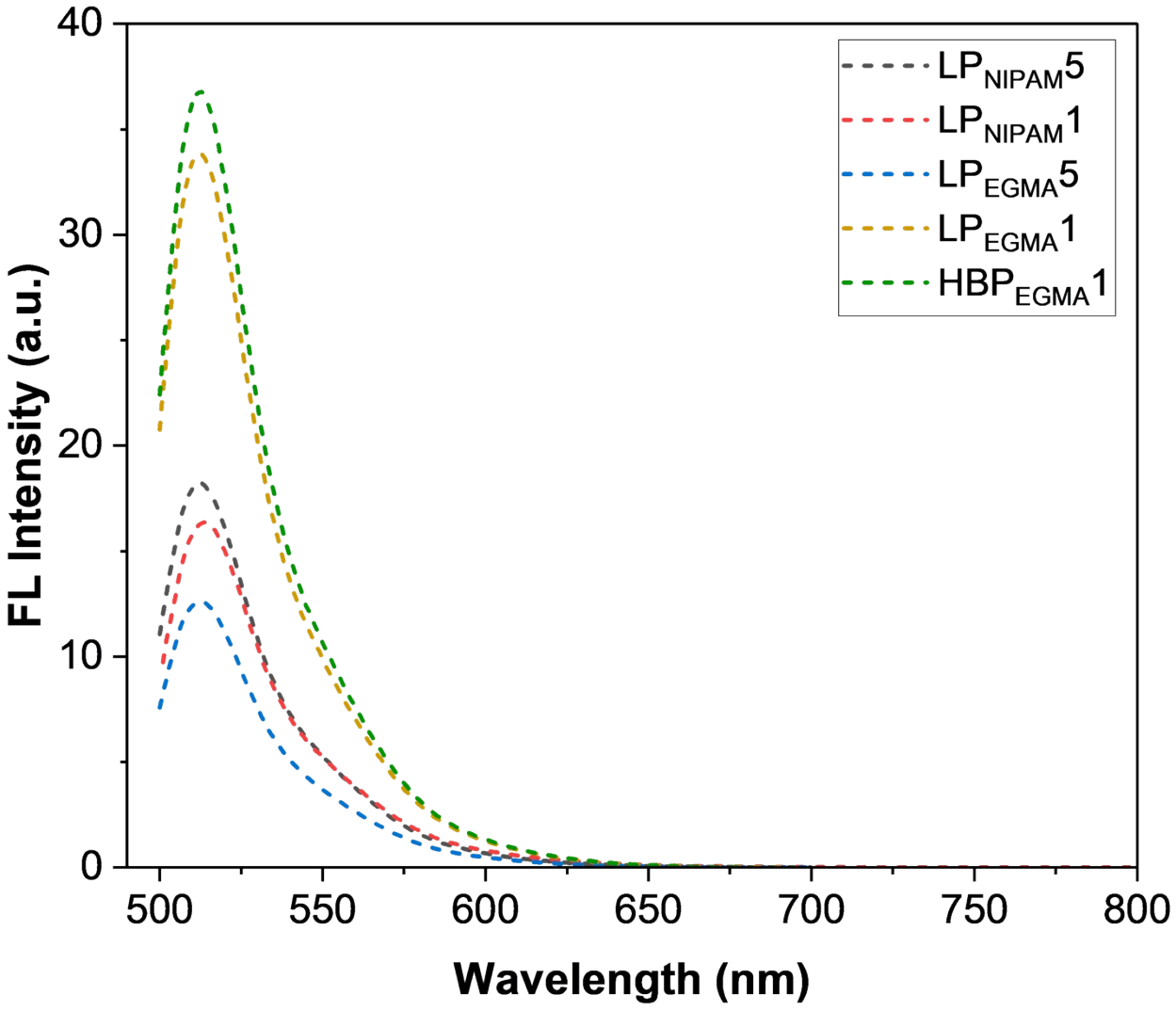

Figure S58. Fluorescence emission spectra of thermoresponsive fluorescent polymers normalized by the effective fluorescein concentration ([FluA]) at a polymer concentration of 0.1 mg mL^{-1}. The entire emission spectrum was divided by the corresponding [FluA] value for each polymer to account for differences in fluorophore loading and enable comparison of intrinsic fluorescence responses across different polymer architectures and compositions.

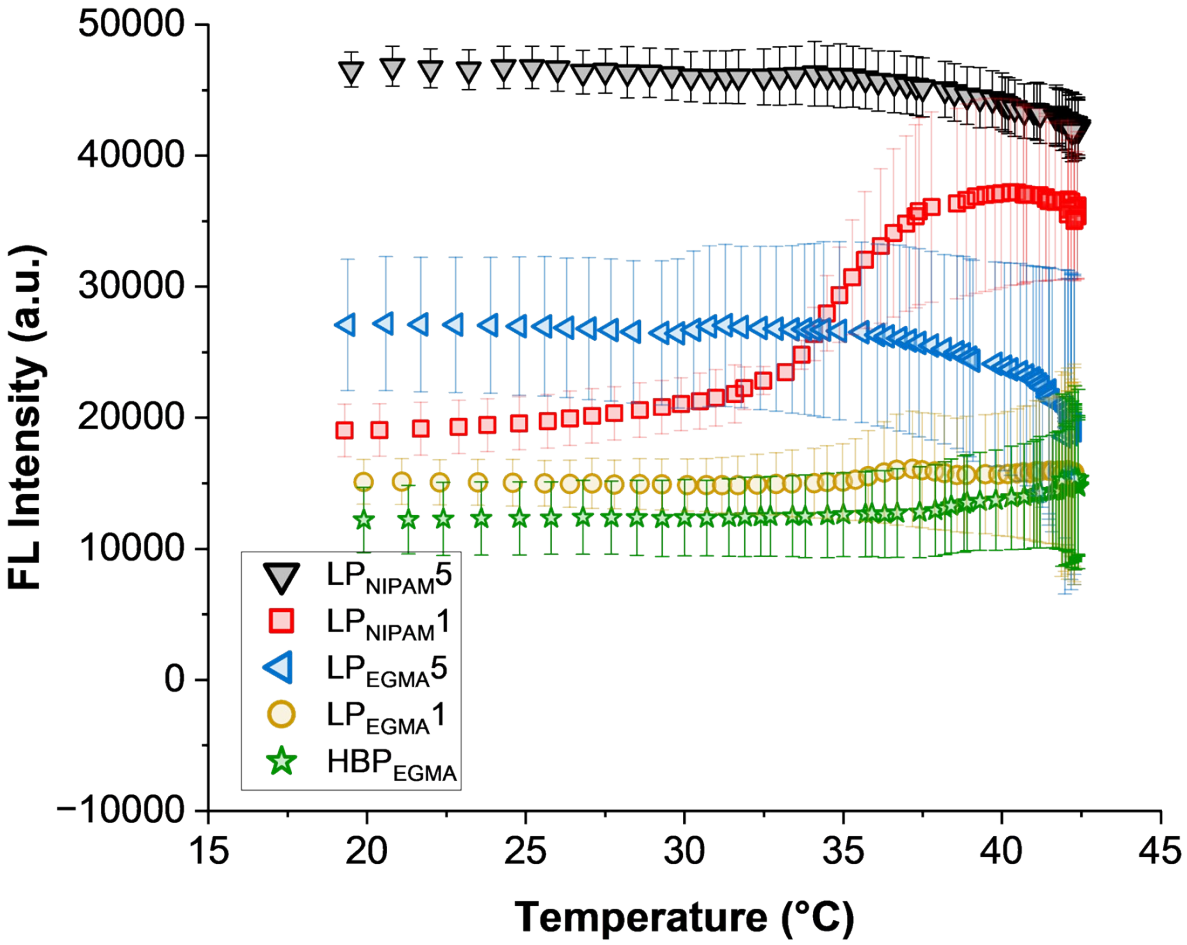

Figure S59. Temperature-dependent fluorescence intensity profiles of NIPAM- and PEGMA-based thermoresponsive fluorescent polymers obtained from emission maxima (λ_{em} = 518 nm). Data points represent the mean of multiple independent measurements, and error bars indicate standard deviation.